The Met Office operational wave forecasting system: the evolution of the Regional and Global models

Nieves G. Valiente[1], Andrew Saulter[1], Breogan Gomez[1], Christopher Bunney[1], Jian-Guo Li[1], Tamzin Palmer[1], Christine Pequignet[1]

[1]Met Office, Fitzroy Road, EX1 3PB, Exeter, UK

Correspondence to: Nieves G. Valiente (nieves.valiente@metoffice.gov.uk)

Abstract. The Met Office operational wave forecasting modelling system ~~is an operational forecast system~~ runs four times ~~daily~~ a day at the Met Office to provide global and regional forecasts up to 7 days ahead. The underpinning model uses a recent development branch of the 3rd generation spectral wave model WAVEWATCH III® (version 7.12) that includes ~~a number of~~ several updates developed at the Met Office. ~~Code contributions~~ These include the Spherical Multiple-Cell (SMC) grid, rotated pole grid formulation for mid latitudes, enhancements to OASIS coupling and updates to the netCDF postprocessing. Here we document ~~and describe~~ the technical details behind the ~~Met Office operational~~ system ~~of WAVEWATCH III® configurations models~~ with a view to further development~~s and special attention to some of the scientific contributions provided~~. We focus on the ~~These include a g~~global (GS512L4EUK) and regional (AMM15SL2) baseline configurations. ~~forecast deterministic model (GS512L4EUK) and two regional models nested one way covering the Northwest (NW) European shelf and UK waters (AMM15SL2) as well as an Atlantic wave ensemble (AS512L4EUK).~~ GS512L4EUK ~~and AS512L4EUK are~~ is based on a ~~four tier~~ multi-resolution four tier SMC 25-12-6-3km grid ~~refinement where currents are not included. The R~~regional~~. AMM15SL2 is run operationally both as a standalone forced model and as the wave component of a two way ocean wave coupled operational system FOAM AMM15. The~~ AMM15SL2 configuration covers the United Kingdom shelf using ~~baseline configuration is based on a two tier SMC grid that is~~ a two tier SMC 3-1.5km grid ~~higher resolution configuration that focuse~~focuses on the shelf seas around the United Kingdom ~~that also~~ (3km resolution) ~~where coastal cells have 1.5km resolution and~~ includes wave-current interaction~~s is included~~. ~~Results from a 2 year hindcast demonstrate the ability of the baseline configurations to reproduce both in situ and satellite wave observations. Model observations correlation is above 0.94-0.96 with standard deviations of differences that correspond to maximum 13-25% of the observed mean bulk wave diagnostics, demonstrating the quality and accuracy of the system.~~ Evidence of resolution dependent differences in wave growth w~~as~~ere observed, leading to slightly overestimated significant wave heights ~~when replicating~~ in coastal mid-range conditions by AMM15SL2, ~~and better suited to replicate the extremes~~but improved representation of extremes compared to GS512L4EUK. ~~Additionally, the inclusion of wave-current interaction in AMM15SL2 tends to larger spread on the observation-model differences. Hence, a~~Additionally, although ~~lthough~~ a positive impact of the surface currents is not always shown in the overall statistics of the significant wave height due to a larger spread i~~o~~n the observation-model differences, ~~the addition of currents~~wave-current effects help to better capture the distribution of the energy in terms of frequency and direction near the coast (>20% improvement), which has implications ~~in~~to beach safety, ~~risk to~~

coastal overtopping risk and shoreline evolution. ~~helps to significantly improve the prediction of the wave direction and period near the coast (>20% improvement), which has implications in beach safety, risk to coastal overtopping and shoreline evolution.~~ Future system developments such as the use of sea point wind forcing, the optimisation of the models in line with model resolution _and_~~,~~ the utilisation of SMC multigrid ~~and data assimilation~~ are discussed.

1 Introduction

Marine monitoring and prediction are crucial for the coastal and offshore sectors~~. Having~~ _and having_ an accurate short range wave forecast is essential in many different ~~marine and coastal~~ applications. A wide range of areas such as marine navigation or offshore industries (e.g., renewable energy offshore farms, fishing, commercial oil and gas extraction) rely on accurate forecasts to ensure a safe and timely functioning of their activities_; and the_ ~~.~~ ~~F~~_f_orecasting of dangerous events that may lead to human and property risk ~~both offshore and at the coast~~ is key for rapid decision making. Numerical weather prediction (NWP) models are used for operational weather and ocean forecasting, providing ~~model~~ outputs to downstream users and forecasters. Met Office NWP systems for ocean forecasting include forecasts of ocean dynamics, waves, storm surges and ecosystems. ~~Hence, Met Office~~_These_ operational ocean forecasting models deliver prediction~~s and monitoring~~ of the marine environment contributing to safety at sea, industry and marine planning among others (Siddorn et al., 2016).

The National Centres for Environmental Prediction (NCEP) community spectral model WAVEWATCH III® (Tolman, 2014), herein WW3, is used operationally in both global and regional model configurations worldwide (e.g., GFSv16 wave (NOAA, 2020)). The Met Office ~~have has developed~~_runs_ an operational system of WW3 _wave forecast_ configurations _and research coupled atmosphere-wave-ocean models (e.g., Lewis et al., 2019; Bruciaferri et al., 2021; Castillo et al., 2022)_ that ~~is~~_are_ based on a recent development branch of the community code (version 7.12). As part of the WW3 Development Group (WW3DG), the Met Office has contributed with several developments to the WW3 codebase, including:

- the Spherical Multiple-Cell (SMC) grid which provides an unstructured multi-resolution (i.e., coarser offshore with higher resolution in coastal waters) spatial grid (Li, 2012) to improve model efficiency and enable improved forecast skill toward coastal zones;
- rotated pole grid formulation for mid latitudes;
- enhancements to the OASIS coupling for compatibility with ocean and atmospheric models;
- and updates to the netCDF postprocessing. These include grid interpolation from SMC to regular grids for products generation, CF compliant netCDF and user configurable netCDF meta-data to maintain consistency with Copernicus Marine service naming conventions.

~~These latest developments have facilitated the migration to version 7.12 of WW3 in~~_are now part of_ wave forecasting operations ~~and in research coupled models including Northwest European shelf (e.g., Lewis et al., 2019; Bruciaferri et al., 2021;~~_)_ ~~) and the Indian regional (Castillo et al., 2022) coupled wave-ocean and atmosphere-wave-ocean research systems.~~ This paper

65 documents the deployment of these recent ~~latest~~ WW3 ~~wave model~~ developments ~~introduced by the Met Office and describes~~in the Met Office ~~WW3-based wave~~ operational wave forecasting system~~s with unstructured multi-resolution which includes a global model and two regional models nested one-way covering the Northwest European shelf and United Kingdom (UK) waters and the Atlantic wave ensemble~~. Particular attention is paid to the impact of resolution and the effect of wave-current interactions ~~in the~~on model accuracy. A description of the operational wave modelling system with focus on the global and

70 regional UK waters baseline configurations is presented in Sect. 2. Methods and data sources for evaluating model performance are presented in Sect. 3. The ~~o~~Operational forecast skill of the system is shown in Sect. ~~4~~4 and ~~and~~ additional assessment o~~n~~f the accuracy of the models ~~Model evaluation performance w~~with a view to further development is described in Sect. ~~3~~5. ~~Model analysis is focused on the global and regional UK waters baseline configurations. Operational forecast skill is shown in Sect. 4.~~ Finally, a discussion~~a summary~~ with key challenges and future work ~~to update the systems~~ and conclusion ~~is~~are presented

75 in Sect. ~~5~~6 and 7, respectively.

2 The Met Office operational wave models

The Met Office operational forecasting system ~~of WW3 configurations~~ (Table 1) includes a global ~~forecast deterministic~~ deterministic configuration ~~model~~ (GS512L4EUK)~~,~~ and two regional configurations, a ~~and~~ regional deterministic ~~models~~ nested one-way covering the Northwest (NW) European shelf and UK waters (AMM15SL2)~~,~~ and ~~as well as~~ an Atlantic wave

80 ensemble (AS512L4EUK) (Fig. 1). AMM15SL2 is run ~~as~~both as a ~~waves~~ standalone wave model (i.e. forced one-way by winds and surface currents) and as the wave component of the FOAM-AMM15 ocean-wave coupled operational system ~~FOAM-AMM15~~ (AMM15 coupled; e.g., ~~Bruciaferri et al., 2021;~~ Lewis et al., 2019) used to produce Copernicus Marine Service products (Saulter, 2020b) from the Northwest Shelf Monitoring and Forecast Centre (NWS-MFC; e.g.: https://marine.copernicus.eu/about/producers/nws-mfc). This section describes the model and baseline configurations:

85 GS512L4EUK and AMM15SL2. For additional information on AS512L4EUK and AMM15 coupled models refer to Bunney and Saulter (2016), and Tonani et al. (2019) and Bruciaferri et al. (2021), respectively.
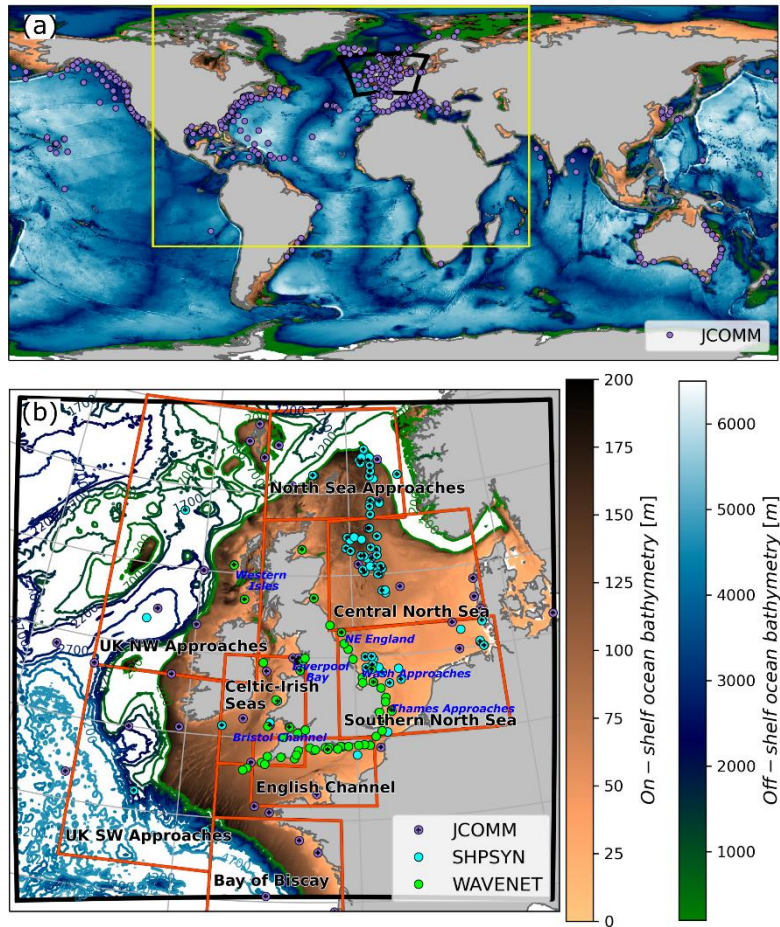
Figure 1. (a) Global and (b) northwest (NW) European shelf – UK waters physical context and model domains. Yellow box and black solid line in (a) indicate the cut-off area for the Atlantic wave ensemble and the NW European shelf – UK waters domains, respectively. (b) NW European shelf – UK waters domain with areas used for analysis indicated in red. In-situ observations are shown as solid dots. In-situ observations include the Joint WMO IOC Commission for Oceanography and Marine Meteorology's operational Wave Forecast Verification Scheme (JCOMM), Ship Synop Ob-servations at fixed platforms (SHPSYN) and UK WAVENET and National Network of Regional Coastal Monitoring Programmes in-situ observations for coastal waters (WAVENET). Locations where there is overlap with JCOMM observations are marked with a cross.

2.1 Research to operations

All mission critical NWP models at the Met Office are run under an operationally maintained supercomputer production system known as the Operational Suite (OS). To maintain consistency and operational resilience, scientific and technical updates to these models follow a prescribed process defined in Parallel Suite (PS) projects, which aim to ensure the successful pull through of scientific improvements of the Met Office's Numerical Weather Prediction Models into the Operational environment (Walters, 2021). For the upstream NWP modelling systems a PS is essentially a copy of the latest operational suite to which scientific and technical updates are applied. The PS is run in parallel with the current Operational Suite on a separate HPC to

4

avoid any resource contention. Once the PS is stable it will be "frozen" and cycled for a 6-8 week period during which verification and performance metrics will be collected. Once all the system performance checks of the PS are concluded this becomes the OS. Both OS and PS are numbered sequentially. The models described here correspond to the latest Met Office operational systems that became operational in May 2022 after Parallel Suite 45 (herein PS45), run in parallel with Operational Suite 44 (hereafter OS44). All these suites are built as a rose suite workflow – a toolkit for writing, editing and running application configurations (http://metomi.github.io/rose/doc/html/index.html, last access: 01 July 2022) – where the model components, configurations and running characteristics are defined. Refer to *Sect. 2.4* for more detail.

2.~~2~~1 ~~Core model~~Model description

The Met Office operational wave forecasting system is based on the WAVEWATCH III® third-generation spectral model (Tolman, 2014) at version 7.12. This model resolves the evolution of the phase-averaged two-dimensional (frequency-direction) wave energy spectrum in time and space using the net effect of sources and sinks of wave energy~~;~~, i.e.~~,~~, a total source term describing local wave energy growth and dissipation, and advection of wave energy through the wave model grid. To enable conservation in the presence of ocean currents, the model describes these changes in terms of wave action (Ardhuin et al., 2012, 2017).~~.~~ The total source term is ~~can be~~ defined ~~as~~by the combination of different physical processes that, in deep waters, can be simplified to ~~the~~a wind-wave interaction term that describes transfer of momentum from the atmosphere to the ocean surface waves, a nonlinear wave-wave interaction term that describes energy transfers between waves of different frequencies, and a dissipation term describing loss of energy from the waves to the surrounding ocean and atmosphere (Valiente et al., 2021a). Additionally, the operational systems include a linear input term ~~for~~used to initial~~i~~se wave growth and parameterizations of ~~additional~~ shallow water processes (i.e., depth-induced breaking and wave bottom interactions). The total source term is therefore defined as:

$$S_{total} = S_{in} + S_{nl} + S_{diss} + S_{bf} + S_{brk}$$

~~WAVEWATCH III®~~WW3 provides multiple options for both source term parameterizations and numerical advection (WW3DG, 2019). This section summarizes the options chosen for the Met Office operational configurations. More details of the compilation switches and source term tuning values can be found in the ~~Refer to *Supplement*~~*Supplementary* Material. ~~for a detailed information of the model source terms parameterisations and the compilation switches.~~

The Met Office operational wave forecasting systems use the Ardhuin et al. (2010) ~~Ardhuin et al. (2010)~~ ST4 package to parameterise wave growth (S_{in}) and dissipation via whitecapping (S_{diss}).~~.~~ The family of parameterisations in ST4 ~~uses a positive part of the wind input~~defines S_{in} based on WAM cycle 4 parameterisation (Janssen, 2004) with an ad-hoc reduction of the wind contribution to account for the impact of long waves on short waves through a tuneable sheltering coefficient (TAUWSHELTER=0.3; refer to Table S2 in ~~*Supplement*~~*Supplementary* material) that decreases the drag coefficient at high winds (Saulter et al., 2017; Valiente et al., 2021a). For compatibility with Met Office Global Unified Model wind forecast data, a minor adjustment on the control of the input wind stress (BETAMAX ~~on~~ namelist value set to~~of~~ 1.39; refer to Table S2 in ~~*Supplement*~~*Supplementary* material) has been implemented across both global and regional wave models. The BETAMAX

value is also adjusted for the ~~particular case~~case of the ocean-wave regional coupled configuration which is forced by ECMWF winds (BETAMAX ~~on~~ namelist value of 1.48; refer to Table S2 in ~~Supplement~~Supplementary material). Input wind stress to S_{in} is derived using conversion from atmospheric model 10m neutral wind speed to momentum stress flux computations which are included in the source term (FLX0); i.e., stress is defined implicitly inside the source terms subroutines. The model assumes

140 neutral atmospheric stability in these calculations. Additionally, a switch with linear wave growth (LN1; Cavaleri and Rizzoli, 1981) for lower winds is implemented (Valiente et al., 2021b), to enable the consistent spin-up of the model from calm conditions and a more accurate description of the initial wave growth.

S_{diss} is parameterised from the wave spectrum saturation following the ~~general~~ ideas of Phillips (1985) with the integrations over directions presented in Ardhuin et al. (2010). The Discrete Interaction Approximation (DIA) package (NL1; Hasselmann

145 et al., 1985) is used to resolve (S_{nl}) nonlinear wave–wave quadruplets interactions that enable downshifting of energy input in the upper tail of the wave spectrum into longer waves. NL1 is developed for deep water, using the appropriate dispersion relation for resonant wave interactions. For shallow water, this source term uses a scaled version of the deep-water dispersion relation.

As part of the shallow water physics, the Met Office wave ~~systems~~model configurations include source terms to resolve depth

150 induced refraction, shoaling and breaking. ~~Hence, The s~~Shallow water wave energy dissipation includes the surf breaking parameterisation proposed by Battjes and Janssen (1978) (DB1) and JONSWAP bottom friction formulation (BT1; Hasselmann et al., 1973). ~~The Discrete Interaction Approximation (DIA) package (NL1; Hasselmann et al., 1985) is used to resolve nonlinear wave–wave quadruplets interactions. NL1 is developed for deep water, using the appropiate dispersion relation in the resonance conditions. For shallow water this source term uses a scaled version of the deep-water dispersion~~

155 ~~relation. Conversion from wind speed to momentum stress flux computations are included in the source term (FLX0); i.e., stress is defined implicitly inside the source terms subroutines. Additionally, a switch with linear wave growth (LN1; Cavaleri and Rizzoli, 1981) for lower winds is also implemented (Valiente et al., 2021b). LN1 allows for the consistent spin up of the model from calm conditions and improves the initial wave growth.~~ Model spectral resolution is identical in all the wave operational systems with 30 frequencies logarithmically spaced between 25 to 1.5 seconds (starting at 0.04118Hz) and 36

160 directional bins that are linearly spaced.

Advection of wave energy through the model grid satisfies the wave dispersion relationship, for which wave energy at lower frequencies will travel more rapidly through the model grid than waves at ~~short~~high frequencies. All configurations of the Met Office operational forecasting system utilise the SMC grid (Li, 2012). One of the key features of this grid is that it allows higher resolution cells in areas of interest (shallow water, coastal areas and islands) whilst maintaining coarse resolution in the

165 open ocean for computational efficiency. The SMC grid retains the quadrilateral cells as in the standard latitude-longitude grid so that simple finite difference schemes could be used. Sub-time-steps are applied on different cell sizes to speed up propagation calculations with a choice of 2nd or 3rd order upstream non-oscillatory (UNO) advection schemes (Li, 2008). The refraction induced wave spectral rotation and the great circle turning are combined and calculated with a re-mapping scheme, which is not subject to the Courant–Friedrichs–Lewy (CFL) restriction but to a physical limit not exceeding the bathymetry

170   gradient direction or a user defined limit angle. Grid cells are merged at high latitudes to relax the CFL restriction and a fixed

     reference direction is used to define wave spectra in the polar region so that the whole Arctic Ocean could be included in the

     global domain. The multi-resolution refinement is useful to resolve small islands and coastline details, which are important in

     ocean surface wave propagations (Saulter et al., 2017). The "*Garden Sprinkler Effect*" (GSE) caused by the discrete directional

     bins of the wave energy spectrum is alleviated with a diffusion term similar to the PR2 option in WW3 model (Booij and

175   Holthuijsen, 1987), plus an optional averaging scheme for further smoothing (WW3DG, 2019).

Table 1 Specifications of the operational production of all the Met Office wave systemsmodels: GS512L4EUK, AS512L4EUK, AMM15SL2 and AMM15 coupled.

		Forecast Run	Update Run
GS512L4EUK	*Forecast length and run frequency*	T+144 for 0ZZ, 12Z T+66 for 6Z, 18ZZ	T+6 for 0Z, 6Z, 12Z, 18Z
	Wind forcing	Hourly NWP global forecast at 10km resolution	Hourly NWP global update at 10km resolution
	Ice forcing	Global OSTIA at 1/12º resolution	Global OSTIA at 1/12º resolution
	Initialisation	Restart file update T+6	Restart file update T+6
	Boundary conditions	--	--
AS512L4EUK	*Forecast length*	T+168	--
	Run frequency and members	00Z/12Z:0-17 members, 06Z/18Z:0,18-34 members	--
	Wind forcing	Hourly NWP MOGREPS-Global forecast atmospheric ensemble at 20km resolution	--
	Ice forcing	Global OSTIA at 1/12º resolution	--
	Initialisation	Restart file update T+6	--
	Boundary conditions	2D spectral boundary conditions at 25 km resolution	--
AMM15SL2	*Forecast length and run frequency*	T+66 for 0Z, 06Z, 12Z, 18Z	T+6 for 0Z, 6Z, 12Z, 18Z
	Wind forcing	Hourly NWP global forecast at 10km resolution	Hourly NWP global update at 10km resolution
	Current forcing	Hourly AMM15 (00Z) at 1.5km resolution	Hourly AMM15 (00Z) at 1.5km resolution
	Initialisation	Restart file update T+6	Restart file update T+6
	Boundary conditions	2D spectral boundary conditions at 25 km resolution	2D spectral boundary conditions at 25 km resolution
AMM15 coupled	*Forecast length*	T+144	--
	Run frequency	00Z	--
	Wind forcing	Hourly ECMWF forecast winds for T0 to T72 3-hourly ECMWF forecast winds for T72 to T144	--
	Initialisation	T-48 hindcast cycle. Restart file T-24	--
	Boundary conditions	2D spectral boundary conditions at 25 km resolution	--
	Hindcast	T-48 using hourly ECMWF winds from previous analysis cycle	--

2.2 Baseline configurations of the operational forecasting system

180 **2.23.1 GS512L4EUK Global Wave Model**

The wave forecast global model configuration GS512L4EUK covers the whole globe from 80° S to 86° N (Fig. 1a) and using model bathymetry is based on GEBCO 2014. The model grid is based on aa four-tier SMC 25-12-6-3km refined grid, for which refinement where the coarsest cells are located in open waters and resolved at approximately 25km (0.35° longitude by 0.23° latitude) in mid-latitudes. The 25-km coarsest cells represent a base resolution equivalent to an N512 atmosphere model

185 and are thensuccessively halved to 12km, 6km and 3km as the grid gets closer to the coastline. The configuration is denoted as GS512L4EUK to represent a base resolution equivalent to N512 atmosphere, the use of the SMC grid with four-tier levels,

8

and the designationAn area of special interest is designated areas in UK waters, where the higher resolutions are is applied more widely (Saulter et al., 2016). This configuration serves as baseline for tThe Atlantic ensemble forecast system for prediction of Atlantic-UK wind waves (AS512L4EUK; Bunney and Saulter, 2015; Saulter et al., 2016) which is based on a cropped version of the GS512L4EUK grid from 25° S to 83° N. Refer to Bunney and Saulter (2015) for a detailed information on the ensemble model.This configuration was first introduced in November 2016 at OS38 (Saulter et al., 2016).
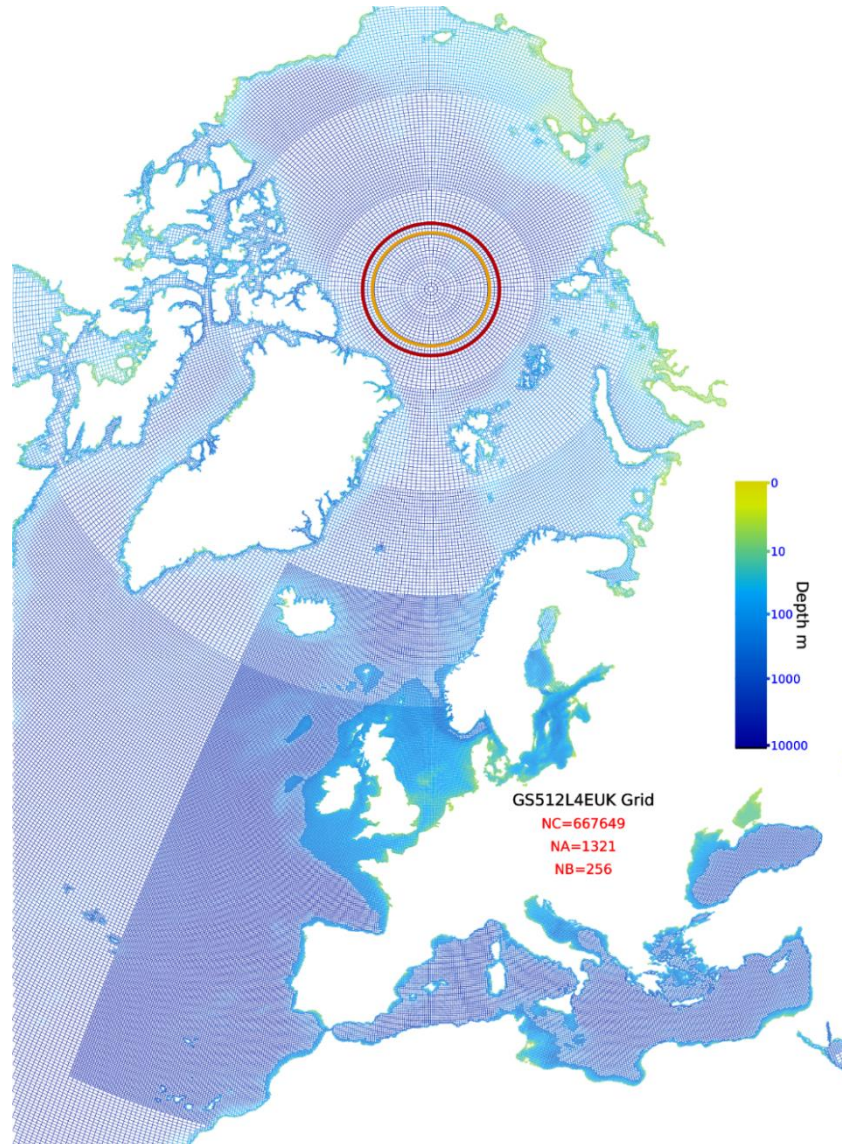
Figure 2. Spherical Multiple-Cell (SMC) GS512L4EUK global model grid across the European-Arctic region. Coarsest (open waters) cells are resolved at approximately 25km in mid-latitudes (0.35° longitude by 0.23° latitude) and reduced by a factor of two to 12km, 6km and 3km. 12km cell size are set over the European region (27N 25W to 68N 42E) with a reduction to 6km for cells with depths less than 320m depth and to 3km for those cells around the UK coastline.

Fig. 2 shows the European-Arctic region of the GS512L4EUK global model grid. ~~The use of the 3km cell refinement has been restricted to waters of the NW European shelf (45° N 16° W to 61.15° N 9.4° E) in order to reduce computational costs. This cell resolution is only applied to coastal waters to best represent the coastal mask (Saulter et al., 2016).~~ Over ~~the wider~~an European~~an~~-wide region (covering approximately 25° W to 27° E and 42° N to 68° N), the coarsest cell size has been set to 12km so that the model can exploit the full detail of the current Met Office global atmosphere-ocean model (approximately 10km resolution), whilst any cells with depths less than 320m are resolved at 6km. This depth was chosen as a threshold to apply higher resolution since wave energy with mean periods of about 18s or longer will begin to interact with the seabed. The use of the 3km cell refinement ha~~s been~~is restricted to ~~waters of~~coastal cells on the NW European shelf (45° N 16° W to 61.15° N 9.4° E) ~~in order to~~to best represent the coastline of the UK (Saulter et al., 2016)~~,~~ whilst minimising ~~reduce~~computational costs. ~~This cell resolution is only applied to coastal waters to best represent the coastal mask (Saulter et al., 2016).~~ At higher latitudes, longitudinal cell sizes are doubled (by a factor of two at 60° N, four at 75° N, eight at 83° N) in order to support a larger CFL time-step than would be permitted by a regular latitude-longitude grid (Li and Saulter, 2014; Saulter et al., 2016). The Arctic part (cells inside golden circle in Fig. 2) is not used in the operational forecast system at present since for most of the time it is covered by sea ice.

The GS512L4EUK model is forced by hourly global atmospheric 10m neutral wind files and ice concentration interpolated to the coarsest resolution of the SMC grid (i.e., 25km). 10m neutral winds are provided by a high-resolution atmosphere-ocean coupled global configuration (Williams et al., 2018) of the Unified Model (UM; e.g., Walters et al., 2019; Brown et al., 2012) and NEMO ocean model each hour~~;~~ ~~. T~~the atmosphere-ocean coupled model has 0.23° longitude by 0.16° latitude resolution (N1280L70; 2560 latitude x1920 longitude and vertical 70 levels), with approximately 10km grid length in mid latitudes. Ice concentration is provided by the Operational Sea Surface Temperature and Sea Ice Analysis (global OSTIA; Good et al., 2020) also produced at the Met Office. ~~Since February 2018 the NEMOVAR data assimilation analysis scheme is used in OSTIA to combine a background (first guess) ice field with daily satellite ice information from the Ocean and Sea Ice Satellite Application Facility (product OSI-401-b) (Good et al., 2020). This observed ice field is gridded using the extended Global ORCA12 grid (ORCA12extL75 tripolar grid at 1/12° resolution with approximately 9km grid length in mid latitudes and 6km near the UK) and concentrations below 10% are set to zero.~~ GS512L4EUK uses simple ice blocking (IC0) where grid points covered by ice are treated as land and a cut-off ice concentration value of 50% at which obstruction ~~begins~~is used. This global model provides full 2D spectral boundary conditions for the nested operational wave (AS512L4EUK, AMM15SL2-UK waters) and AMM15 ocean-wave coupled configurations.

~~GS512L4EUK provides full 2D spectral boundary conditions for the nested operational wave and ocean-wave coupled configurations. Hence, AS512L4EUK, AMM15SL2 and ocean-wave coupled AMM15 regional models are nested one-way with lateral boundary conditions supplied from the global wave model (forced by UM neutral global winds at 10km spatial resolution and 1-hourly) interpolated to the coarsest resolution of the SMC grid (i.e., 25km). Wave boundary data are supplied as wave spectra onto the outer boundaries.~~

2.3.2 AMM15SL2 NW shelf-UK Waters Wave Model

The UK waters wave model, herein referred to as AMM15SL2, covers the NW shelf-UK area from approximately 45° N 20° W to 63° N 12° E with a resolution of 3-1.5km. The domain extends beyond the shelf break in order to take boundary conditions in open waters which are not subject to shallow water processes, but is primarily focused on forecasting the shelf seas around the UK; i.e., Celtic and Irish Seas, North Sea, and English Channel (Fig. 1b). The AMM15SL2 configuration name is derived from the AMM15 (1.5km NW Shelf Atlantic Margin Model) ocean model that encompasses the same region and the use of a two-level SMC grid refinement (Li, 2011) with variable resolution based on both proximity to coast and water depth (Saulter et al., 2017; Valiente et al., 2021b). This regional configuration was first introduced in November 2018 at OS40.

The grid resolution is of 3km for water depths larger than 40m and 1.5km for coastal cells with water depths of less than 40m (Fig. 2). The SMC grid is based on a rotated north pole at 177.5° E 37.5° N, achieving an evenly spaced mesh around UK. Bathymetry and coastal masking for this configuration are the same as the 1.5km AMM15 NEMO (Nucleus for European Modeling of the Ocean; Madec, 2008) based ocean configuration (Tonani et al., 2019; Graham et al., 2018). Bathymetry and land-sea mask are based on the European Marine Observation and Data Network (EMODnet portal, September 2015 release) corrected to mean sea level (Tonani et al., 2019).

AMM15SL2 is the baseline configuration used for the UK waters wave-only and AMM15 ocean-wave coupled models. Similar to GS512L4EUK, AMM15SL2 wave-only is driven by hourly NWP 10m neutral winds from the global UM-NEMO

operational system and . AMM15SL2 is also forced by hourly currents from the regional AMM15 Ocean-Wave Coupled Model shelf seas Forecast Ocean Assimilation Model (AMM15-FOAM; Tonani et al., 2019, see next Sect. for a summary of

265   details) interpolated in time and space to .

All forcing conditions in the wave standalone models are interpolated in time and space to the underlying coarsest 3km cell resolution regular grid version of the SMC.

The coupled version of this configuration is AMM15 ocean-wave coupled operational forecast system used or the production of CMEMS Copernicus products for the NW shelf domain and differs from the AMM15SL2 UK waters wave model in the

270   forcing sources, being driven by sSurface (10m) wind data at approximately 9km resolution are provided from the atmospheric high-resolution global configuration of the Integrated Forecast System run at the European Centre for Medium-Range Weather Forecasts (ECMWF; https://www.ecmwf.int/en/forecasts/documentation-and-support).. Thise system consists of a WW3 wave model is two-way coupled to the ocean NEMO model AMM15-FOAM using the Ocean Atmosphere Sea Ice Soil (OASIS-MCT coupler; Valckle et al., 2015) coupling libraries. The coupling configuration passes atmosphere to ocean stress, calculated

275   by the wave model, from wave-to-ocean, and surface currents from ocean-to-wave. The ocean component integrates a NEMO physical ocean model and the Nucleus for European Modelling of the Ocean data assimilation system (NEMOVAR; e.g., King et al., 2018; Waters et al., 2015). NEMOVAR uses a 3D-Var first guess at appropriate time (FGAT) scheme which includes bias corrections scheme for both sea surface temperature and altimeter data. Surface (10m) wind data at approximately 9km resolution are provided from the atmospheric high-resolution global configuration of the Integrated Forecast System run at the

280   European Centre for Medium-Range Weather Forecasts (ECMWF; https://www.ecmwf.int/en/forecasts/documentation-and-support). This is 25km resolution for winds and ice in GS512L4EUK and AS512L4EUK; and 3km resolution for winds and currents in AMM15SL2.

2.3.4 AMM15 Ocean-Wave Coupled Model

285   The Met Office AMM15 ocean-wave coupled operational forecast system for the NW shelf consists of a WW3 wave model two-way coupled to the ocean NEMO model AMM15-FOAM using the Ocean Atmosphere Sea Ice Soil (OASIS-MCT coupler; Valckle et al., 2015) coupling libraries. The ocean component consists of the NEMO physical ocean model and the Nucleus for European Modelling of the Ocean data assimilation system (NEMOVAR; e.g., King et al., 2018; Waters et al., 2015). NEMOVAR uses a 3D-Var first guess at appropriate time (FGAT) scheme which includes bias corrections scheme for

290   both sea surface temperature and altimeter data.

Domain, grid and bathymetry of the wave component of this forecast system are the same than for the waves standalone AMM15SL2 UK Waters Wave Model. AMM15 ocean-wave is used in the production of CMEMS Copernicus products for the NW shelf domain and differs from AMM15SL2 UK waters wave model in the forcing sources. Surface (10m) wind data are provided from the atmospheric high-resolution global configuration of the Integrated Forecast System run at the European

295   Centre for Medium-Range Weather Forecasts (ECMWF; https://www.ecmwf.int/en/forecasts/documentation-and-support).

Temporal resolution is hourly up to T+72 and 3-hourly from T+72 to T+144. The wind field is defined on an approximately 9km resolution. As per the other SMC based configurations, ECMWF wind forcing is pre-processed and interpolated to the level of the coarsest wave model cells, equivalent to approximately 3km. Surface current effects on the waves are included, and surface zonal and meridional current fields from the 1.5km North-West Shelf FOAM-AMM15 model are passed as coupled fields every hour since OS44. The coupled surface currents are interpolated directly to the SMC grid sea-points, i.e. at the 3km and 1.5km cell resolutions as appropriate (Saulter, 2020b).

2.34 Operational production

Operationally, GS512L4EUK and AMM15SL2 wave models run ~~operationally~~ four cycles per day (00Z, 06Z, 12Z and 18Z; Table 1) to T+66. The 00Z and 12Z cycle on each day are extended to a 144hour forecast for ~~the case of~~ GS512L4EUK. Both GS512L4EUK and AMM15SL2 are initialised using the restart file T+6 from a short 6hour "update cycle" using the most up-to-date NWP winds. This way all models ~~which include data assimilation.~~ provide a forecast that it is initialised with the best available descriptions for atmosphere and ocean (i.e., with as many observations assimilated as possible).

~~The operational setup of the wave model does not include data assimilation (Saulter et al., 2020a). However, this is partially accounted for by GS512L4EUK and AMM15SL2 configurations being run in two separate modes: a forecast run and an update run. The forecast suite produces the short-medium range forecasts using NWP forecast winds. This suite also produces the operational products. The update suite re-runs a short 6hour update cycle using the most up-to-date NWP assimilated winds. This update cycle provides the best possible start conditions for the next forecast cycle. Additionally, i~~Ice concentration from global OSTIA for GS512L4EUK, and currents from AMM15-FOAM for AMM15SL2 are updated once a day at 00Z. ~~In practisedeed, t~~The AMM15SL2 wave at 00Z runs before the ocean-wave coupled AMM15 00Z in the Met Office production cycle, forcing ~~to~~ this cycle to use ~~as input file~~ the forecasted currents from the previous day's AMM15 ocean-wave model cycle (i.e., currents at T+24 from previous cycle of AMM15 coupled). The AMM15 ocean-wave coupled model runs once a day triggering a 144hour forecast. Each model cycle starts with a T-48 hours hindcast prior to each forecast. Refer to Saulter (2020a) and Tonani et al. (2021) for more ~~detailed~~ information on the production cycle of CMEMS AMM15 ocean-wave coupled.

AS512L4EUK wave ensemble currently runs as a "lagged" ensemble: members 0 to 17 run to full length (168hour) at 00Z and 12Z whereas members 0 and 18 to 34 run at 06Z and 18Z. A full 36 member lagged ensemble is made up at each cycle from overlapping full length members.

3 Observations and metrics for model accuracy

~~hereaftertie, , hereafter (hereafter) areWave and wind parameters are assessed for the years 2019 and 2020.~~ Modelled ~~W~~waves and winds are evaluated using significant wave height (H_s), mean zero up-crossing period (T_{02}) and mean wave direction (Dir) for the waves, and 10m height wind speeds (U_{10}) and wind direction (U_{10} dir) for the wind forcing conditions. These parameters

13

are widely used for model evaluation as they give information concerning~~of~~ the ~~wave~~ model performance in ~~various~~ aspects such as bulk energy imparted to the ocean surface waves and representation of the wave energy distribution through the frequency domain and directional space. ~~H_s is representative of the bulk energy imparted to ocean surface waves from the atmosphere whereas evaluation of T_{02} helps to assess the ability of the model to represent the wave energy distribution through the frequency domain of the wave spectrum mainly on higher frequencies (i.e., T_{02} is computed using the second spectral moment). Finally, assessment of the wave direction helps to understand the ability of the model to reproduce the distribution of wave energy in the directional space~~ (Saulter A., 2020b).

Wave parameters from the model simulations are assessed using four different datasets: (i) 6/12-hourly in-situ data from the Joint WMO-IOC Commission for Oceanography and Marine Meteorology's operational Wave Forecast Verification Scheme (Bidlot et al., 2007), hereafter JCOMM-WFVS, for H_s and T_{02}; (ii) hourly Daily Ship Synoptic Observations at fixed platforms for H_s and T_{02} across the NW shelf, hereafter SHPSYN; (iii) hourly UK WAVENET and National Network of Regional Coastal Monitoring Programmes (NNRCMP) in-situ observations for coastal waters comprising Waverider buoy measuring H_s, T_{02} and Dir, hereafter WAVENET; and (iv) global satellite merged altimeter data (hereafter MA_SUP03) including JASON 2, CryoSat and SARAL AltiKa H_s data. Wind forcing conditions (U_{10} and U_{10} dir) are verified using JCOMM-WFVS, SHPSYN and MA_SUP03 datasets.

Basic metrics for model evaluation are described in *Supplementary material*. These include *bias*, root mean square deviation (*RMSD*), observations (*SDobs*) and model standard deviation (*Sdmodel*), Pearson correlation coefficient (*r Pierson*), standard deviation of the error (*StdE*), covariance (*Cov*), and variance (*Var*). Extreme verification and extra metrics for model evaluation are also provided and include Scatter Index (*SI*) and Symmetric Slope (*SS*) between the model and the observations. *SI* is calculated dividing the standard deviation of model-observation differences and *Sdobs*. The *SS* is described as the ratio of model variance to observations variance. *Bias* and *RMSD* are used to document the forecast accuracy whereas all the metrics are presented for the model evaluation.

4 Forecast performance

The quality of the Met Office short range forecasting system is evaluated by runnin~~Model evaluation is focused on~~g and verifying the two baseline global (GS512L4EUK) and regional (AMM15SL2) UK waters (refer to Fig. 1a,b) configurations ~~.~~ during 50 days in summer (from 20190619 to 20190814; JJA) and winter (20191204 to 20200124; DJ). These experiments (Table 2) replicate the operational configurations described in *Sect. 2.2*. Initial conditions for FCST experiments used the corresponding T+6 restart output file generated during the analysis experiments (previously run). For comparison purposes, AMM15SL2-FCST was run up to T+144 as per GS512L4EUK-FCST, as opposed to T+66 used in operations. It is noted that currents used as forcing were not available~~lacking~~ in the last 78 hours of the AMM15SL2-FCST runs.

Table 2 Experiments specifications for forecast capability.

Experiment	Description
GS512L4EUK-FCST	JJA (20190619 to 20190814) and DJ (20191204 to 20200124) forecast run global. Forcing: forecast 10km hourly NWP winds and updated fraction of sea ice. Restart at T+6 T+144 forecast at 00Z cycle
AMM15SL2-FCST	JJA (20190619 to 20190814) and DJ (20191204 to 20200124) forecast. Forcing: forecast 10km hourly NWP winds and AMM15 FOAM analysis and forecast hourly currents. Restart at T+6 T+144 forecast at 00Z cycle

360 Forecast skill, from T+24 hours to T+144 hours, ~~across the NW shelf area from T+24 hours to T+144 hours~~ of wind and wave parameters across the NW shelf area over the summer months of JJA and the winter months of DJ for the two baseline configurations is presented in Fig. 3. Winds tend to be overestimated in both configurations during most of the forecasting period up to T+96 (GS512SL4EUK and AMM15SL2 *biases* are 0.4–0.6 and 0.1–0.3ms^{-1}, respectively; Fig. 3a). ~~Further inside the~~At longer forecast lead times, winds appear to be slower versus the first forecast days, and the tendency is to show a reduced

365 *bias* that might be also associated with compensating ~~ancellation~~ errors (*biases*=0.1 and -0.2 ms^{-1} for GS512SL4EUK and AMM15SL2 at T+144). This is also observed in H$_s$ biases where values are also slightly overestimated (*biases*=0.1 and 0.2m for GS512SL4EUK and AMM15SL2) and model-observation differences are smaller during the winter months (0.02 and 0.1m for GS512SL4EUK and AMM15SL2, respectively; Fig. 3c).

Despite the bias reduction ~~due partially to cancellation errors~~ observed in U$_{10}$ and H$_s$, the forecast skill of both configurations

370 ~~is steady in space, which~~ decreases with lead time (i.e., positive trend) and is slightly weaker during the winter months for both forcing and wave bulk parameters (i.e., U$_{10}$, U$_{10}$ dir, H$_s$ and T$_{02}$), suggesting a consistent behaviour across model resolution. The decrease in the forecast skill appears to be relatively steady for the first four days of forecast (U$_{10}$ *RMSD*=1.5–2.5ms^{-1} and H$_s$=0.1-0.4m up to T+96 in JJA; Fig. 3b,d); however, *RMSD* trend indicates a more rapid decrease in the forecast skill after these (increases to 3.5ms^{-1} and 0.6m at T+144). It is noted that the degree of decrease in the forecast skill for the case of T$_{02}$ is

375 smaller compari~~ng~~ed with H$_s$ and, in fact, values of both *bias* (-0.8s and -0.5s for GS512SL4EUK-FCST and AMM15SL2-FCST, respectively; Fig. 3g) and *RMSD* (1.4s and 1.1s for GS512SL4EUK-FCST and AMM15SL2-FCST, respectively; Fig. 3h) are almost constant for the first four days in both JJA and DJ (Fig. 3g,h) periods.
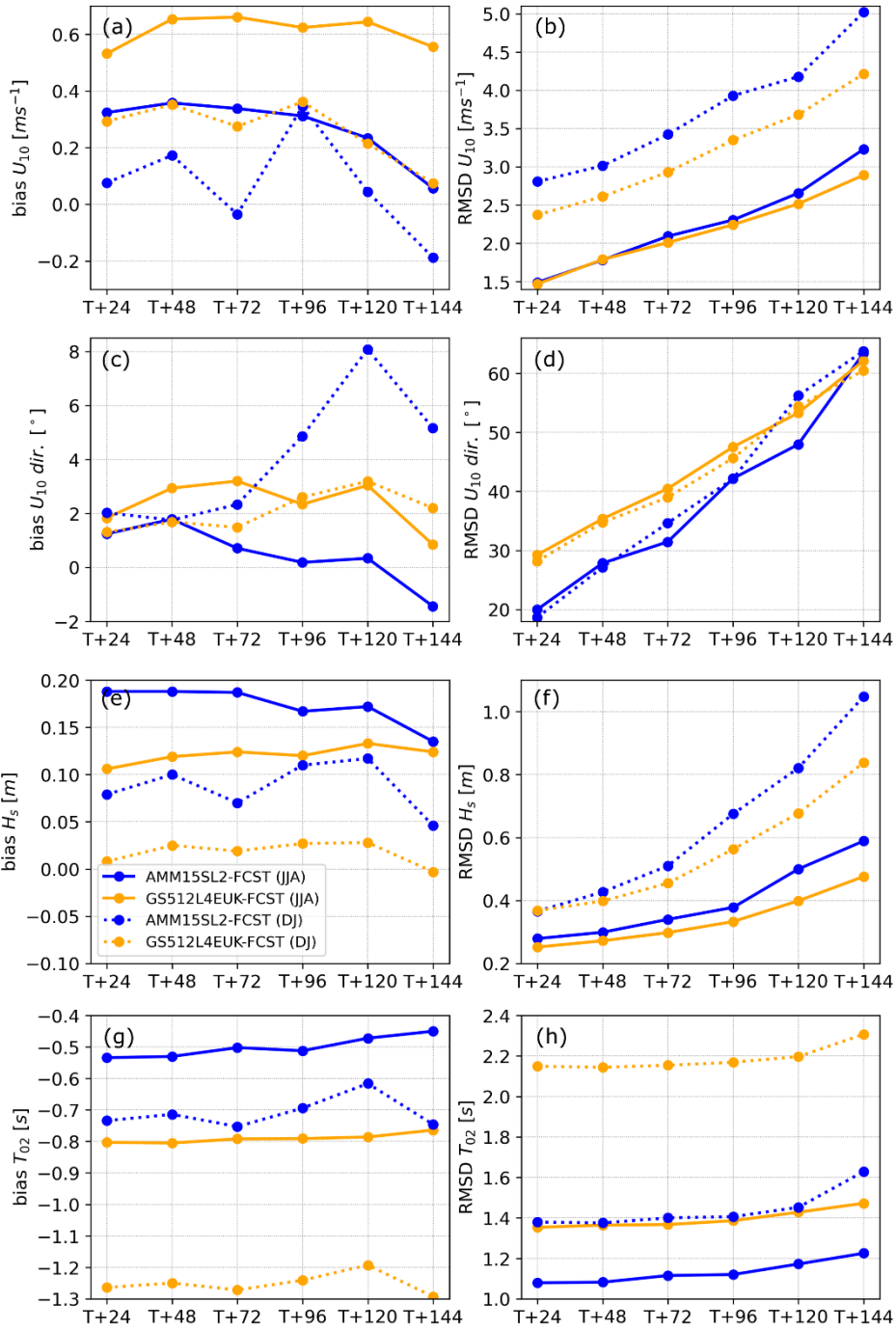
Figure 3. Forecast (a,c,e,g) *bias* **and (b,d,f,h) root mean square deviation (*RMSD*) for wind speed (U_{10}; a,b), wind direction (U_{10} dir; c,d), significant wave height (H_s; e,f) and mean period (T_{02}; g,h) every 24 hours over a forecast period of 6 days (T+144) for the area of the NW shelf. Values are averaged over the months June-July-August (JJA; solid lines) and December-January (DJ; dotted lines) and correspond to the NW shelf – UK waters model (AMM15SL2-FCST; blue) and the global model (GS512L4EUK-FCST; orange).**

Model forecast skill ~~reproducing~~for H_s suggests that the positive impact of including the surface currents and having increased resolution is not always shown in the overall statistics.~~,~~ ~~and i~~Indeed, H_s *bias* and *RMSD* for the regional baseline configuration during the forecast period are greater (AMM15SL2-FCST *RMSD*=0.3-1m) than for the global (GS512SL4EUK-FCST *RMSD* =0.2-0.8m) model (Fig. 3d). Conversely, AMM15SL2-FCST shows a better performance with a decrease in bias and >20% reduction in *RMSD* compared to the global configuration for T_{02} (Fig. 3g,h). Forecast skill differences are associated with a better representation of bathymetric features, depth related processes and wave-current interaction present in AMM15SL2. ~~Investigation on t~~The overall contribution of each of these factors is~~n~~ ~~presented~~investigated in the next section.~~Given the focus in this paper on describing the accuracy of a widely used operational wave forecasting system with a view to further development, investigation on the overall contribution of each of these factors is presented in Model evaluatio~~*n*

~~AS512L4EUK wave ensemble currently runs as a "lagged" ensemble due to limitations in resource (for both the Atlantic wave ensemble and the driving MOGREPS Global atmospheric ensemble). At each run cycle, 17 members and the control run to full forecast length with lead times out to 168hour whilst the other 17 members do a short 6hour cycle to maintain continuity. The full length members alternate at each cycle. Hence, members 0 to 17 run at 00Z whereas members 0 and 18 to 34 run at 06Z and 18Z. A full 36 member lagged ensemble is made up at each cycle from overlapping full length members from the current and previous cycles.~~

~~The AMM15 ocean-wave coupled runs once a day triggering a 144hour forecast. Each model cycle starts with a T-48 hours and does a 2day hindcast prior to each forecast. Initial conditions are taken at T-24. The role of the hindcast is to have a forecast that it is initialised with the best available descriptions for atmosphere and ocean (i.e., with as many observations assimilated as possible). High frequency wind forcing during the hindcast part of each cycle are constructed from the previous ECMWF analysis cycle. Refer to Saulter (2020a) and Tonani et al. (2021) for more detailed information on the production cycle of this system.~~

5~~3~~ Model evaluation

The focus of this paper is to evaluate some of the physical aspects of our operational ~~model~~system in detail. Assessment of the ~~, which is done in this section based on long analysis runs. The previous section~~forecast performance showed that the model has a consistent behaviour across lead times, with a degradation in performance that is mostly explained by the wind forcing data. ~~This suggests that a model forced with analysis winds will be representative of the performance at different lead times making this a valid platform to study these features.~~

We now investigate the performance characteristics of the baseline configurations with a specific focus on the influence of spatial resolution and wave-current interactions using long analysis runs (#AN), herein GS512L4EUK-AN and AMM15SL2-AN (Table 3). ~~This suggests that a model forced with analysis winds will be representative of the performance at different lead times making this a valid platform to study these features. Model evaluation is focused on global (GS512L4EUK) and regional~~

(AMM15SL2) UK waters (refer to Fig. 1a,b) configurations. Verification of the systems will be used to document the performance characteristics of the baseline configurations, with a view to further development with a specific focus on the influence of spatial resolution and wave current interactions. For a detailed evaluation of AMM15 Ocean Wave Coupled

420 Model and AS512L4EUK wave ensemble refer to Saulter (2020b) and Bruciaferri et al. (2021), and Bunney and Saulter (2015), respectively. Performance of the baseline configurations was validated using hindcast analysis experiments (#AN), herein GS512L4EUK-AN and AMM15SL2-AN (Table 32). Trials covered the period from 1st January 2019 to 31st December 2020 and were based on daily cycles of the models forced by NWP 10km resolution hourly operational update cycle winds, between T+0 and T+6 (4 cycles/day), and OSTIA the updated fraction of sea ice fraction (GS512L4EUK-AN) and AMM15 FOAM

425 1.5km sea surface currents (AMM15SL2-AN). The trials were initialised from rest with a 10day spin-up period that was discarded. Each cycle used the restart file at T+24 from the previous cycle. Lateral wave spectral boundary conditions for the AMM15SL2-AN simulation were supplied from the GS512L4EUK-AN simulation. For a detailed evaluation of AMM15 Ocean-Wave Coupled Model and AS512L4EUK wave ensemble refer to Saulter (2020b), and Bruciaferri et al. (2021), and Bunney and Saulter (2015), respectively. The spectral boundary conditions are provided as external files and interpolated to

430 the 3km resolution outer boundaries.

Table 32 Experiments specifications for model evaluation.

Experiment	Description
GS512L4EUK-AN	2-year (20190101 to 20201231) analysis run global Forcing: Operational archived hourly NWP 10km resolution updated winds and updated fraction of sea ice. Restart at T+24
AMM15SL2-AN	2-year (20190101 to 20201231) analysis run regional UK waters Forcing: Operational archived hourly NWP 10km updated winds and AMM15 FOAM updated currents. Restart at T+24

5Wave parameters from the model simulations are evaluated using four different datasets: (i) 6/12 hourly in-situ data from the Joint WMO IOC Commission for Oceanography and Marine Meteorology's operational Wave Forecast Verification Scheme (Bidlot et al., 2007), herein JCOMM WFVS; (ii) hourly Daily Ship Synop Observations at fixed platforms across the NW

435 shelf (hereafter SHPSYN); (iii) hourly UK WAVENET and National Network of Regional Coastal Monitoring Programmes (NNRCMP) in-situ observations for coastal waters comprising Waverider buoys (simplified as WAVENET); and (iv) global satellite merged altimeter data (MA_SUP03) including JASON 2, CryoSat and SARAL AltiKa data. Wind forcing conditions were verified using JCOMM WFVS, SHPSYN and MA_SUP03 datasets. Wave and wind parameters are assessed for the years 2019 and 2020.

440 Different wave and wind parameters are evaluated depending on the observation type (i.e., different observation types measure different parameters): significant wave height (Hs), mean zero up-crossing period (T02) and mean wave direction (Dir) for the waves and 10m height wind speeds (U10) and wind direction (U10 dir) for the wind forcing conditions. These parameters are widely used for model evaluation as they give information of the model performance in various aspects. Hs is representative

18

of the bulk energy imparted to ocean surface waves from the atmosphere whereas evaluation of T02 helps to assess the ability of the model to represent the wave energy distribution through the frequency domain of the wave spectrum mainly on higher frequencies (i.e., T02 is computed using the second spectral moment). Finally, assessment of the wave direction helps to understand the ability of the model to reproduce the distribution of wave energy in the directional space (Saulter A., 2020b). Basic metrics for model evaluation are described in Supplement material. These include bias, root mean square deviation (RMSD), observations (SDobs) and model standard deviation (SDmodel), Pearson correlation coefficient (r Pierson), standard deviation of the error (StdE), covariance (Cov) and variance (Var). Extreme verification and extra metrics for model evaluation are also provided and include Scatter Index (SI) and Symmetric Slope (SS) between the model and the observations. SI is calculated dividing the standard deviation of model-observation differences and SDobs. The SS is described as the ratio of model variance to observations variance.

3.1 Global spatial and temporal model accuracy Wind forcing

Metrics for U_{10} and U_{10} dir against JCOMM-WFVS, SHPSYN and MA_SUP03 observations (Table 3) are computed for the individual domains in order to assess the consistency of these for both configurations. Interestingly, differences in U_{10} metrics are not significant, indicating that forcing conditions are steady and suggesting that the wind interpolation to the underlaying regular grid with the coarsest SMC resolution (25km for GS512L4EUK and 3km for AMM15SL2) does not degrade the overall wind speed performance. However, U_{10} dir compare closer to observations for the AMM15SL2 domain (RMSD=21.49º and 17.00º, StdE=21.46º and 16.98º for GS512L4EUK and AMM15SL2 respectively) demonstrating that errors between modelled U_{10} dir and observations are both smaller and more representative of the wind conditions across the NW shelf. This highlights that wind interpolated to the AMM15SL2 3km retaining the original spatial variability of 10km performs better in terms of U_{10} dir.

Global spatial and temporal forcing accuracy is tested evaluated using altimeter MA_SUP03 observations Global wind speed (U_{10}) verification statistics versus satellite observations (Fig. 4 MA_SUP03) which provides measurements of wind speed and wave height. The main observed feature is that are presented in Fig. 3. there is an U underestimation of observed wind speeds by the model (Fig. 4c,d) occurs in those areas that present either very small or strong mean wind speeds (Fig. 3 4a,b), and whilst overestimation occurs in mid latitudes regions with modal observed mean wind conditions (5–10ms⁻¹). Areas which present the lowest mean wind conditions are those across equatorial and close mid latitude regions during both summer and winter months. These areas with present the smallest very small wind variability (SD mean values are of O.0.6 ms⁻¹; Fig. 4 3g e,h f) where overall RMSD mean values are of O.0.6 ms⁻¹ (Fig. 3g,h). Underestimation in these areas seems to be partially linked to average mean speeds of 5ms⁻¹ or lower (i.e., calm wind conditions) possibly also associated to sampling bias from the satellite for observations calm wind conditions. Additionally, v Very energetic areas such as the Southern part of the Pacific Ocean also present negative bias throughout the year, but these are more exacerbated during JJA months (Fig. 3 4c; winter in the Southern Hemisphere) during which the largest mean winds are registered. Equally, negative bias is present in the northern part of the Atlantic Ocean also corresponding with the strongest winds (average U_{10}>10ms⁻¹) during DJF northern hemisphere

19

winter months (Fig. ~~4~~3d). As expected, these areas with the strongest winds also present the largest $SDmodel$ (>2ms^{-1}) and $RMSD$ (1.2ms^{-1}). ~~Positive~~ ~~bias during both JJA and DJF always occur in mid-latitudes of both hemispheres. This wind overestimation corresponds with modal observed mean wind speeds (5–10ms^{-1}). Largest overestimation rates are observed in~~

480 ~~those mid latitudes closest to the equatorial strip with negative bias.~~

Variability for ~~Similar to the forcing conditions,~~ wave metrics ~~variability~~ match the variability ~~o~~nf the wind~~ave~~ field~~, t~~. ~~This is:is~~such that larger values of $bias$, $RMSD$ and $SDmodel$ always correspond with areas with the strongest average wave conditions. A ~~Certain~~ $bias$ seasonality is observed with waves underestimated across areas affected by tropical and intra-tropical storms; i.e., tropical, mid and high latitudes in the northern hemisphere during DJF (Fig. 5b,d,f,h) and Indian Ocean

485 during JJA (Fig. 5a,c,e,g). This negative $bias$ during stormy seasons turns into a positive one of the same order during periods with calmer average conditions (Fig. 5c,d). Conversely, the southern part of the South Pacific Ocean shows a large variability in the $bias$ with no clear seasonality, possibly due to ~~cancellation~~ompensating errors. H$_s$ values of $RMSD$ oscillate between 0.1–0.3m in most parts of the globe, with a substantial increase to 0.5–0.6m in those areas with the largest mean wave conditions and ~~larger~~variability ~~deviations~~ about ~~from~~ the mean values (i.e., Southern Ocean during JJA and North Atlantic

490 and North Pacific during DJF). Additional large positive biases around island chains and ice edges are also present, which we attribute to a combination of misrepresentation errors from observation and model. On the one hand, ~~t. It~~it is acknowledged that satellite measurement errors are larger in complex coastlines and, on the other hand, model resolution and misplacements in the extension of ice sheets will yield in position errors in the wave field~~; however, this overestimation is consistently present throughout the year and is not observed in other coastlines, suggesting that it is more a limitation associated with the model~~

495 ~~configuration than with observation uncertainties~~. Adopting the GS512L4EUK SMC configuration helped reduc~~ing~~e such biases ~~from~~compared to previous configurations (Saulter et al., 2016); however, biases in these areas are still likely due to issues with land/ice masking and the representation of fetch in the model grid.

~~As expected, model seasonal variability is shown in the verification metrics with largest values of SDmodel (>2ms⁻¹) and~~

~~RMSD (1.2ms⁻¹) across those areas which present the strongest winds (Fig. 3a,b), southern Pacific Ocean during JJA and~~
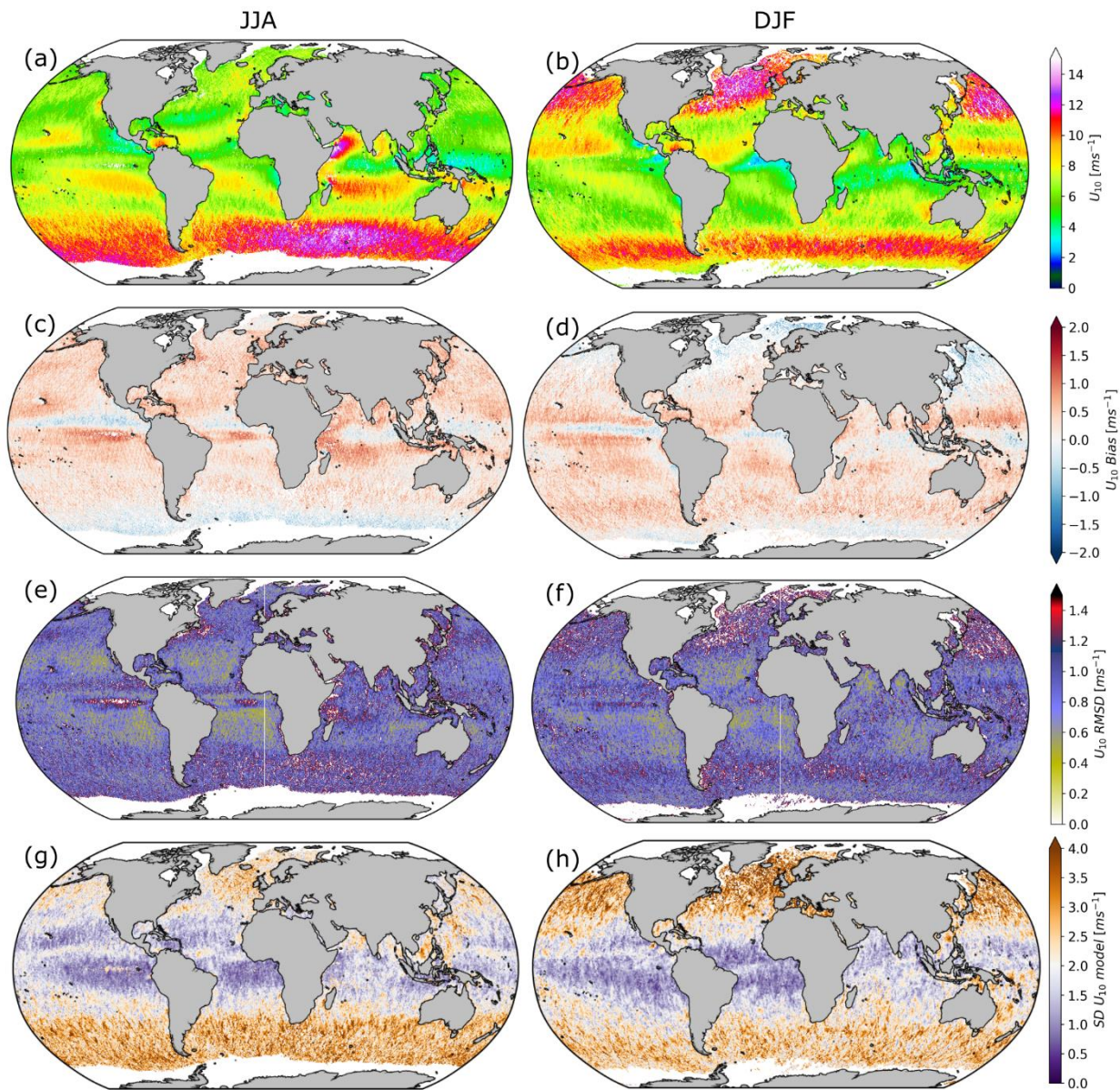
500 ~~northern Atlantic Ocean during DJF.~~

Figure 4̶3̶. (a,b) Mean, (c,d) *bias* **and (e,f) root mean square deviation (***RMSD***)** between wind (U₁₀) forcing conditions and merged altimeter observations (MA_SUP03), **and (g,h) model standard deviation (***SDmodel***)** ~~between wind (U₁₀) forcing conditions and merged altimeter observations (MA_SUP03)~~ **across the global domain for GS512L4EUK-AN. Stats are aggregated every 15-days and averaged for the months June-July-August (JJA; left column) and December-January-February (DJF; right column).**
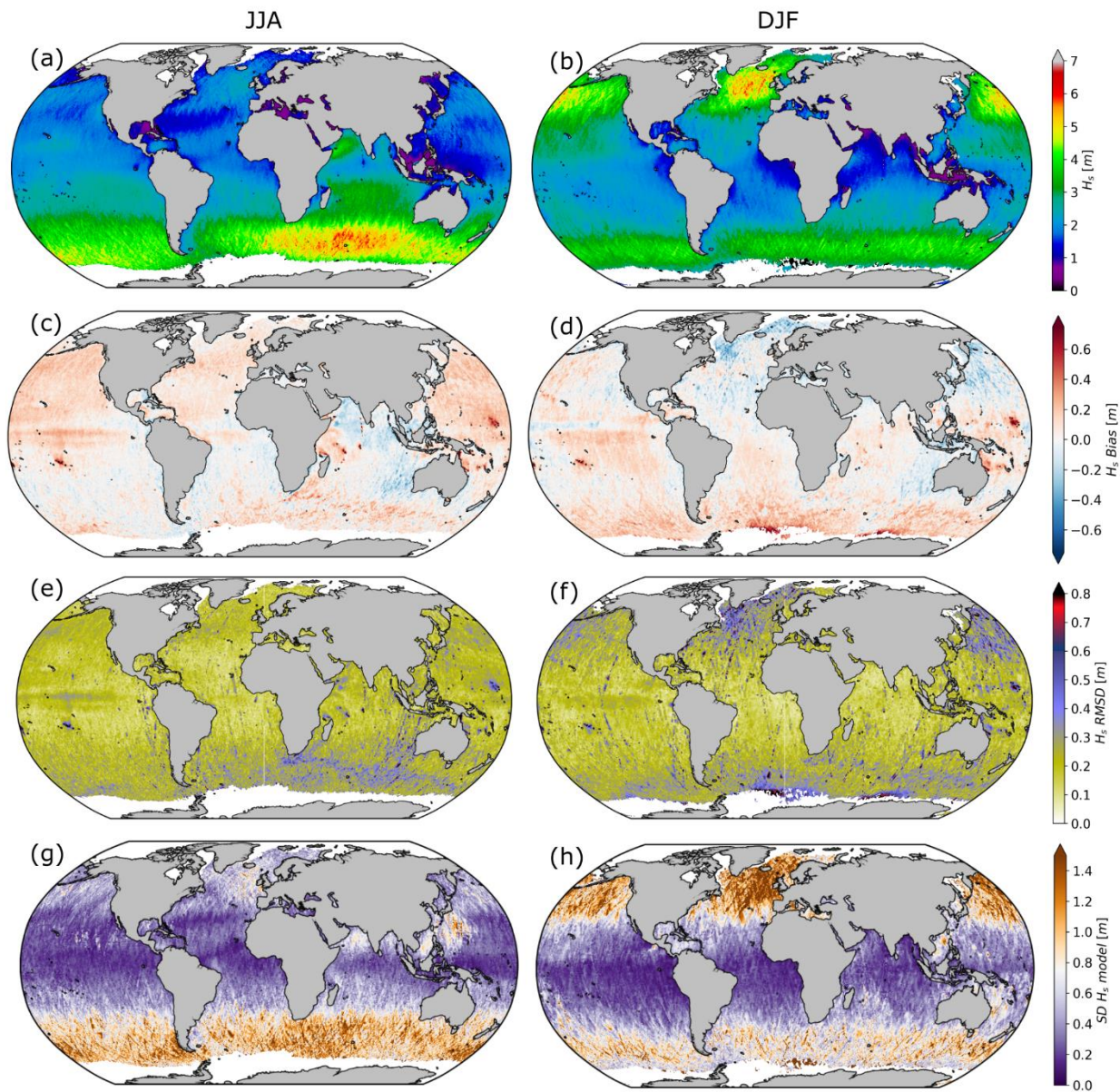
Figure 5. (a,b) Mean, (c,d) *bias* and (e,f) root mean square deviation (*RMSD*) between modelled significant wave height (H$_S$) and merged altimeter observations (MA SUP03), and (g,h) model standard deviation (*SDmodel*) across the global domain for GS512L4EUK-AN. Stats are aggregated every 15-days and averaged for the months June-July-August (JJA; left column) and December-January-February (DJF; right column) over 2019-2020.

Model calibration is based on the best overall performance skill. Figs. 4 and 5 suggest some imbalance during swell dominated conditions in areas such as the Southern Pacific Ocean and the Indian Ocean where winds over this period appear overpredicted whereas significant wave height is consistently underestimated (e.g., waters approaching Western Australia; Fig. 5c,d). Something similar, albeit to a lesser extent, occurs in tropical and mid latitudes in the western part of the North Atlantic where,

22

515 despite a slight overestimation of the forcing conditions, the model shows a negative *bias* with respect to altimeter observations. ~~This imbalance between forcing conditions and model response requires further tuning and/or nesting to improve swell energy propagation from the Southern Ocean for those specific regions..~~

5.2 Regional spatial and temporal model accuracy

Assessment of AMM15SL2-AN modelled H_s and T_{02} against in-situ observations across the UK waters is presented in Fig. 6.
520 Analysing in-situ observations individually allows us to get a more detailed understanding of caveats on the model performance in the different areas of analysis. Although some metrics variability between summer and winter months ~~is observed~~, overall, T_{02} seems to be consistently underestimated in most locations (*bias*=-0.5s; Fig. 6g,h) whereas H_s is slightly overestimated (*bias*=0.1–0.2m, Fig. 6e,f). Following the seasonal pattern observed in the global domain, AMM15SL2 model performance is slightly weaker (i.e., larger values of *bias* and *RMSD*) when waves are larger (i.e., DJF). However, conversely to the other
525 metrics, the correlation between model and observations (*r*) is improved during the winter months (average *r* >0.92 versus 0.88 during JJA) suggesting that AMM15SL2 struggles more to replicate the wave energy in the frequency domain during lower energy conditions (H_s=1–2m, T_{02}=5–6s; Fig. 6a–d). Spatially, there are some specific locations where mean *bias*, *RMSD* and *StdE* statistics are consistently larger throughout the year (e.g., buoys in the Bristol and English Channels and coastal buoys in very sheltered areas). Whilst the model shows some skill in these regions, the high variability characterised by strong
530 currents due to the tidal range (hypertidal in the case of the Bristol Channel), linked to the fact that those locations are very close to the coast and some local features (e.g., headlands, highly spatially variable bathymetry with features of <3–1.5km spatial scale) are not fully represented by the model, which make these regions very dynamic and difficult to resolve more accurately with the current model configuration.
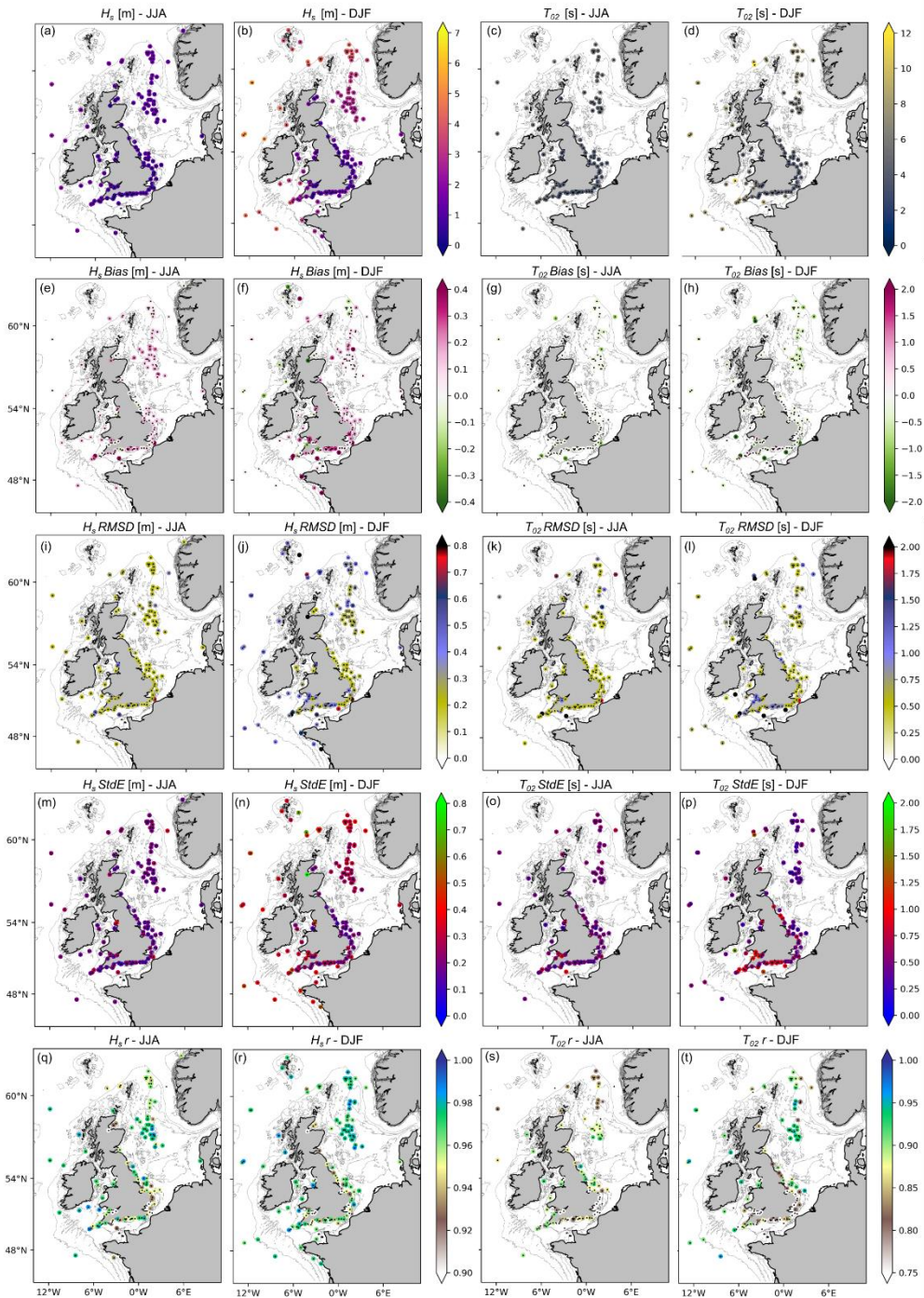
Figure 6. (a–d) Mean, (e–h) *bias*, (i–l) root mean square deviation (*RMSD*), (m–p) standard deviation of error (*StdE*) and (q–t) Pearson correlation coefficient (*r*) between modelled significant wave height (H_s) and mean zero up-crossing period (T_{02}) and in-situ observations across the UK waters domain for AMM15SL2-AN. Stats are computed for the months June-July-August (JJA; left

24

column) and December-January-February (DJF; right column) over 2019–2020. Observations included are JCOMM-WFVS, SHPSYN and WAVENET.

540 ~~35.3.2 Wave bulk statistics~~Comparison of configuration performance

The relative importance of wind and current inputs is presented through evaluations comparing GS512L4EUK-AN and AMM15SL2-AN trials against all observations (i.e., WAVENET, JCOMM-WFVS, SHPSYN and MA_SUP03; Table 3). Overall metrics are computed for the individual domains, i.e. ~~being~~ the entire globe and the NW shelf – UK waters area respectively. Note that evaluation of wave direction (Dir) only corresponds to the coastal waters of the UK.

545 ~~The relative importance of wind and current inputs is presented through evaluations comparing GS512L4EUK-AN and AMM15SL2-AN trials against all observations (i.e., WAVENET, JCOMM-WFVS, SHPSYN and MA_SUP03). Summary statistics for significant wave height (H_s) and mean zero up-crossing period (T_{02}) and wave direction (Dir) are presented in Table 3. Overall metrics are computed for the individual domains being the entire globe and the NW shelf – UK waters area respectively. Note that evaluation of wave direction (Dir) only corresponds to the coastal waters of the UK.~~

550 **Table 3. Summary statistics for wind speed (U_{10}), wind direction (U_{10} dir), significant wave height (H_s), mean zero up-crossing period (T_{02}) and wave direction (Dir): GS512L4EUK-AN and AMM15SL2-AN versus observations of WFVS, SHPSYN, WAVENET and merged altimeter (MA_SUP03) over 20190101 to 20201231.**

		GS512L4EUK-AN						AMM15SL2-AN					
Variables	Observations	Mean	Bias	RMSD	StdE	SS	r	Mean	Bias	RMSD	StdE	SS	r
U_{10}	WFVS	7.19	0.26	2.00	1.98	1.13	0.86	8.27	0.20	2.20	2.19	1.06	0.84
	SHPSYN	8.19	0.34	1.63	1.59	0.97	0.92	8.19	0.34	1.62	1.58	0.97	0.92
	WAVENET	-	-	-	-	-	-	-	-	-	-	-	-
	MA_SUP03	7.87	0.26	1.49	1.46	1.05	0.92	8.47	0.36	1.36	1.31	1.09	0.95
U_{10} dir	WFVS	-	0.83	23.05	23.04	0.99	-	-	0.49	14.36	14.36	1.01	-
	SHPSYN	-	-1.32	19.92	19.88	0.99	-	-	-1.27	19.65	19.61	0.99	-
	WAVENET	-	-	-	-	-	-	-	-	-	-	-	-
	MA_SUP03	-	-	-	-	-	-	-	-	-	-	-	-
H_s	WFVS	1.88	0.05	0.29	0.29	0.95	0.97	2.08	0.09	0.28	0.26	0.95	0.98
	SHPSYN	2.09	0.12	0.33	0.31	0.93	0.97	2.09	0.12	0.32	0.30	0.91	0.97
	WAVENET	1.25	0.02	0.32	0.32	1.02	0.94	1.25	0.06	0.26	0.25	0.99	0.96
	MA_SUP03	2.74	0.05	0.35	0.35	0.95	0.97	2.71	0.02	0.32	0.32	0.93	0.98
T_{02}	WFVS	6.31	-0.80	1.41	1.16	0.60	0.79	6.15	-0.56	0.99	0.82	0.62	0.88
	SHPSYN	5.98	-0.58	0.99	0.80	0.71	0.86	5.98	-0.56	0.98	0.80	0.69	0.87
	WAVENET	4.52	-0.24	0.78	0.74	1.19	0.86	4.52	-0.12	0.67	0.66	1.15	0.89
	MA_SUP03	-	-	-	-	-	-	-	-	-	-	-	-
Dir	WFVS	-	-	-	-	-	-	-	-	-	-	-	-
	SHPSYN	-	-	-	-	-	-	-	-	-	-	-	-
	WAVENET	-	-0.01	32.79	32.79	0.97	-	-	-1.55	27.58	27.54	0.97	-

25

One of the main factors that influence the reliability of a wave spectral model is the accuracy of the forcing conditions. Modelled wind forcing is compared against observations in order to assess their consistency for the baseline configurations (Table 4). Interestingly, differences in U_{10} metrics are not significant, indicating that wind forcing conditions are steady and suggesting that the wind interpolation to the underlaying regular grid with the coarsest SMC resolution (25km for GS512L4EUK and 3km for AMM15SL2) does not degrade the overall wind speed performance. However, U_{10} dir compares closer to observations for the AMM15SL2 domain (*RMSD*=21.49⁰ and 17.00⁰, *StdE*=21.46⁰ and 16.98⁰ for GS512L4EUK and AMM15SL2 respectively) demonstrating that errors between modelled U_{10} dir and observations are both smaller and more representative of the wind conditions across the NW shelf. (i.e., when the original spatial variability of the 10km winds is retained and not upscaled). ~~Both configurations show good agreement with satellite altimeter observations and in situ observations of Hs. Analysing the observations as a whole (average values), the model and observations present correlation coefficients (Pearson *r*) in the range of 0.94 0.97 and 0.96 0.98 with small *biases* 0.06m and 0.07m for GS512L4EUK AN and AMM15SL2 AN, respectively. Standard deviations of differences between the models and the observations (*StdE*) are 0.32 and 0.28 which correspond to 13 25% of the observed mean Hs. Mean *SS* are 0.95 0.96 indicating that the *SDobs* is larger than *Sdmodel* in both configurations. Although T02 is well reproduced both across the global and the regional domains, mean correlation coefficients are better across the UK waters (i.e., for AMM15SL2 AN): 0.84 for GS512L4EUK AN versus 0.88 for AMM15SL2-AN. There is a tendency to underestimate observed T02 in about -0.54 -0.41s and equally to *r*, mean values of *RMSD* and *StdE* are smaller across the UK waters: *RMSD* = 1.06s and 0.88s and *StdE* = 0.90 and 0.76 for GS512L4EUK AN and AMM15SL2 AN, respectively. Dir metrics show an overall reduction of *RMSD* and *StdE* for AMM15SL2 AN (32.8⁰ for GS512L4EUK AN versus 27.5⁰ for AMM15SL2 AN) suggesting that currents modulation of the wave field and the increased resolution (3km versus 1.5km) help to better capture the wave direction near the coast where bathymetric changes and coastal obstructions are better resolved by the AMM15SL2 configuration. A further contribution to the improved wave direction fields in AMM15SL2 is expected from the wind interpolation as noted in Sect. 3.1.~~

~~Model results from GS512L4EUK AN are compared against satellite observations (MA_SUP03) in Fig. 4. Similar to the forcing conditions, metrics variability match the variability on the wave field. This is: larger values of bias, RMSD and SDmodel always correspond with areas with the strongest average wave conditions. Certain bias seasonality is observed with waves underestimated across areas affected by tropical and intra tropical storms; i.e., tropical, mid and high latitudes in the northern hemisphere during DJF (Fig. 4b,d,f,h) and Indian Ocean during JJA (Fig. 4a,c,e,g). This negative bias during stormy seasons turns into a positive one of the same order during periods with calmer average conditions (Fig. 4c,d). Hs in other areas, such as the west coast of Australia, appear systematically underestimated (bias = 0.2 0.4m). The southern part of the South Pacific Ocean shows a large variability in the bias with no clear seasonality, possibly due to cancellation errors. Hs values of RMSD oscillate between 0.1 0.3m in most parts of the globe, with a substantial increase to 0.5 0.6m in those areas with the largest mean wave conditions (i.e., Southern Ocean during JJA and North Atlantic and North Pacific during DJF). This same~~

585 ~~pattern is observed in SDmodel (Fig. 4g,h) where larger deviations from the mean values coincide with areas where mean Hs is 4m or larger. Additional large positive biases around island chains and ice edges are also present. It is acknowledged that satellite measurement errors are larger in complex coastlines; however, this overestimation is consistently present throughout the year and is not observed in other coastlines, suggesting that it is more a limitation associated with the model configuration than with observation uncertainties. GS512L4EUK SMC configuration helped reducing biases from previous configurations~~
590 ~~(Saulter et al., 2016); however, biases in these areas are still likely due to issues with land/ice masking and the representation of fetch in the model grid.~~

~~Model calibration is based on the best overall performance skill. All configurations in the Met Office wave forecast system~~
~~include the same source term tuning parameters (refer to Supplement material) as this has been found to be suitable in previous~~

28

system versions. Figs. 3 and 4 suggest some imbalance during swell dominated conditions in areas such as the Southern Pacific Ocean and the Indian Ocean where winds over this period appear overpredicted whereas significant wave height is underestimated (e.g., waters approaching Western Australia; Fig. 4c,d). Something similar, albeit to a lesser extent, occurs in tropical and mid-latitudes in the western part of the North Atlantic where, despite a slight overestimation of the forcing conditions, the model shows a negative bias with respect to altimeter observations. This imbalance between forcing conditions and model response requires further tuning and/or nesting to improve swell energy propagation from the Southern Ocean for those specific regions.

Assessment of AMM15SL2-AN modelled Hs and T02 against in-situ observations across the UK waters is presented in Fig. 5. Analysing in-situ observations individually allows us to get a more detailed understanding of caveats on the model performance. Hence, following the seasonal pattern observed in the global domain, a weaker performance (i.e., larger values of bias and RMSD) of the model reproducing Hs is expected when waves are larger (i.e., DJF). Correlation coefficients for Hs are above 0.95 (Fig. 5q,r) and, conversely to the other metrics, r is improved overall during DJF. This improvement in r is even more significant for T02 across the North Sea where r >0.92 on average during DJF, versus 0.88 during JJA. Metrics values suggest a good performance of AMM15SL2-AN; however, the model seems to struggle more to replicate the wave energy in the frequency domain during lower energy conditions (Hs=1-2m, T02=5-6s; Fig. 5a-d). Additionally, T02 seems to be consistently underestimated in most locations (bias=-0.5s; Fig. 5g,h) whereas Hs is slightly overestimated (bias=0.1-0.2m on average). Although metrics variability between summer and winter months is observed, bias, RMSD and StdE statistics at some specific locations are consistently larger throughout the year (e.g., buoys in the Bristol and English Channels). Whilst the model shows some skill in these regions, the high variability characterised by strong currents due to the tidal range (hypertidal in the case of the Bristol Channel), the fact that those locations are very close to the coast and some local features (e.g., headlands, highly spatially variable bathymetry with features of <3-1.5km spatial scale) are not fully represented by the model make these regions very dynamic and difficult to resolve more accurately with the current model configuration.

Differences in model skill replicating in-situ observations suggest some platform dependence, especially for the SHPSYN dataset that includes a variety of buoys, lightvessels and fixed platforms. Inspection of the statistics suggests that when using SHPSYN, model versus observations differences increase 10-30% with respect to model comparisons with other observational data and that this is consistent for both model configurations. This suggests that it is not a problem related to the model performances but with the SHPSYN dataset itself. This issue with the observation quality control procedures has been previously identified in Saulter et al. (2016), where the authors mentioned some metadata inconsistencies such as the sampling time for wave variables and/or type of period data returned by particular platforms.
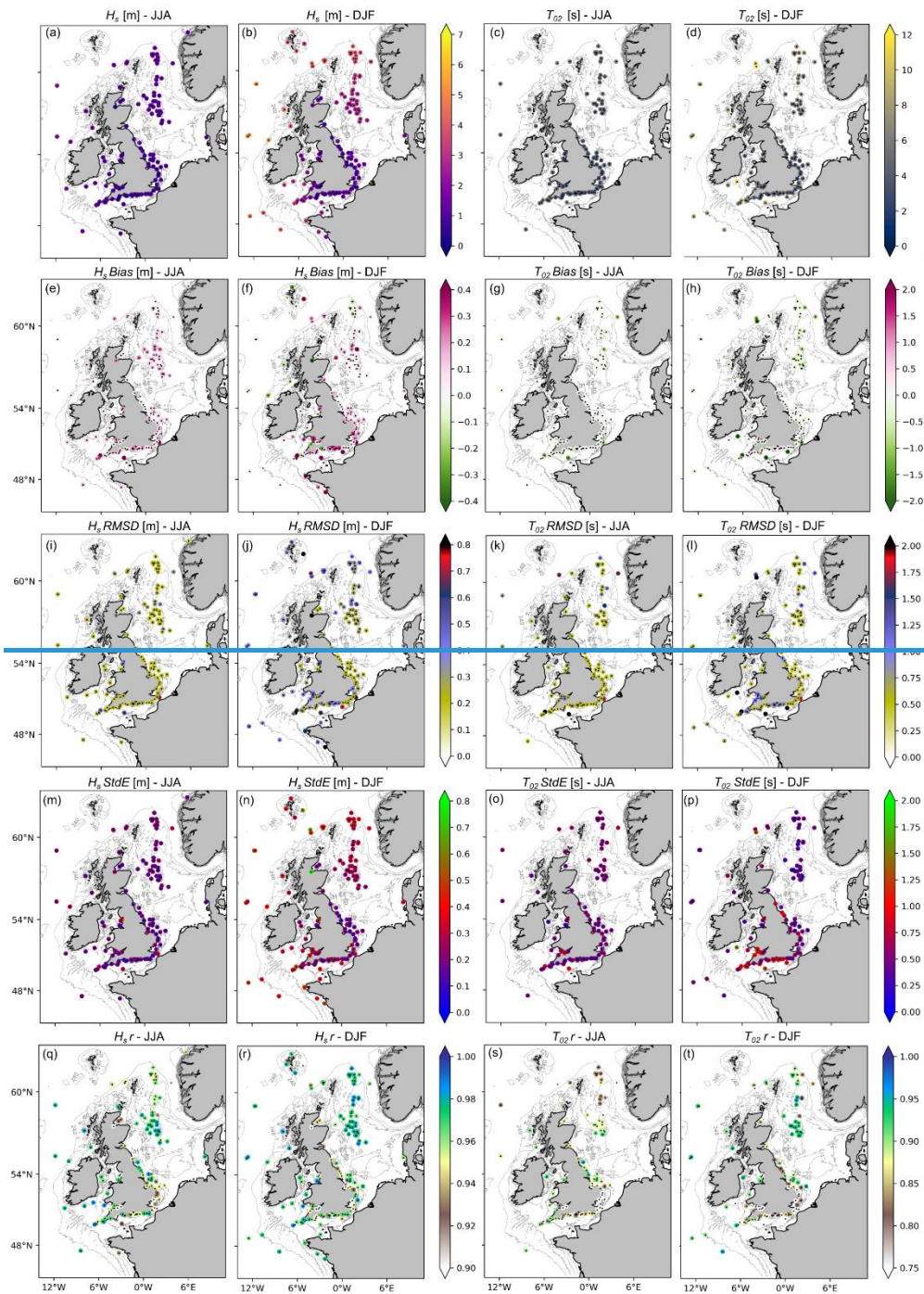
29

Figure 5. (a–d) Mean, (e–h) bias, (i–l) root mean square deviation (RMSD), (m–p) standard deviation of error (StdE) and (q–
t) Pearson correlation coefficient (r) between modelled significant wave height (Hs) and mean zero up-crossing period (T02)

30

and in-situ observations across the UK waters domain for AMM15SL2-AN. Stats are computed for the months June-July-August (JJA; left column) and December-January-February (DJF; right column) over 2019-2020. Observations included are JCOMM-WFVS, SHPSYN and WAVENET.

3.3 Comparison of configuration performance

635 Computation of relative changes in absolute bias and RMSD as well as differences in model capability to replicate the observations (Cov, Var and mean square deviation; MSE) is used to assess differences in performance between the different configurations for the NW shelf – UK waters area. Although the different system configurations use the same tuning of the source terms; GS512L4EUK and AMM15SL2 differ in domain resolution (higher resolution for AMM15SL2 configuration) and the inclusion of surface currents as forcing (for AMM15SL2 configuration).

640 The use incorporation of ocean surface currents in the wave model tends aims to improve modelled sea states (e.g., Hersbach and Bidlot, 2008; Palmer and Saulter, 2016; Ardhuin et al., 2017; Alday et al., 2021 2022). Analysing the observations as a whole (average values), statistics show excellent model accuracy predicting H_s even when currents are not included (i.e., GS512L4EUK). Both baseline configurations present very good correlation coefficients (H_s $r=0.94–0.97$ and T_{02} $r =0.84–0.88$ for GS512L4EUK-AN and AMM15SL2-AN, respectively; Table 3), mean SS (0.95–0.96; i.e., SD_{obs} is larger than SD_{model})

645 and small positive *biases* for H_s (0.06m and 0.07m) and negative for T_{02} (*bias* = -0.54–-0.41s). When comparing differences in performance only for the NW shelf – UK waters (Fig. 7), However, results show that although there is a positive impact of the surface currents and increased resolution, with 5% MSE decrease in coastal locations (i.e., WAVENET, Fig. 7), this the positive impact of the surface currents and increase in resolution is not always prese shown t in the overall statistics of H_s, when comparing the global and the regional configurations and. Hence, n neutral changes and even some degradation in H_s overall

650 performance e exists in specific locations with (overall 1 and 5% increase in *MSE* and *bias* MSE skill change for coastal areas.).

The increased resolution in AMM15SL2, together with the refraction produced by tidal currents, help to better capture mean period and wave direction near the coast where bathymetric changes and coastal obstructions are better resolved (Fig. 7). AMM15SL2-AN shows an acceptable performance in all the coastal areas of analysis with Dir *RMSD* values oscillating from

655 17°–32° which corresponds to 25% of the observation standard deviation. This percentage in the *RMSD* increases to 36% for the case of GS512L4EUK-AN. A further contribution to the improved wave direction fields in AMM15SL2 is also expected from the wind interpolation. Model accuracy improvement for T_{02} is more than 2–9% on average *MSE* and *bias* (Table 3) with >20% reduction in *RMSD*. This overall improvement in the mean period for AMM15SL2-AN is even more significant in most coastal locations with despite some exceptions such as the Scarweather directional wave buoy (Bristol Channel) where,

660 although the tidal modulation of the wave field is only captured by AMM15SL2-AN, it leads to a larger spread o in the observation-model differences. This is related to a lag between the model and observations and a potential double penalty effect in the verification as a result, as well as possible compensation cancellation errors in GS12L4EUK-AN. Previous studies

demonstrated that metrics based on direct point matchup between model data and observations might often lead to the double penalty effect (Crocker et al., 2020), where features are correctly predicted but misplaced with respect to the observations.

665 Other skill changes in H_s between model baseline configurations are <2% (not shown). A more significant impact is observed in the mean period with overall improved skill in replicating T_{02} when both currents and a high-resolution configuration are introduced, i.e., AMM15SL2-AN. This is more than 25% and 10% improvement in T_{02} *MSE* and *bias*, respectively, by AMM15SL2-AN with respect to GS512L4EUK-AN (not shown).

The distribution in relative change between AMM15SL2-AN and GS512L4EUK-AN using all in situ observations in each
670 area of analysis (Fig. 1b) across the UK waters during 2019-2020 is presented in Fig. 6. Following the same pattern as the overall differences in configuration performance, most of the skill changes in H_s can be considered neutral with some outliers: degradation of H_s by AMM15SL2-AN in *MSE* and *bias* (e.g., around 5% across the Bay of Biscay and 1-2% across the English Channel and the Celtic-Irish Seas). Observed T_{02} is significantly better reproduced by AMM15SL2-AN in all areas of analysis except the North Sea Approaches, where difference in skill change is < 1% (i.e., slight degradation by AMM15SL2-AN).
675 Positive skill changes in T_{02} *bias* and *MSE* for AMM15SL2-AN exceed 25% (improvement) in those areas in the south of the domain (Bay of Biscay and SW approaches) where there is a combination of off-shelf and on-shelf in-situ observations. It is important to mention that T_{02} observations in these areas are scarcer when comparing with other parts of the domain, which might lead to unrealistic assumptions. Although T_{02} skill change is still positive for AMM15SL2-AN in the other parts of the domain, skill change differences are reduced and oscillate between 2-9%. When analysing relative changes breaking down
680 per location (Fig. 7), those areas where some degradation of AMM15SL2-AN is observed with respect to GS12L4EUK-AN (Fig. 6) often result from a negative change at a single observations location whilst other locations in the sub-domain see little or no change.
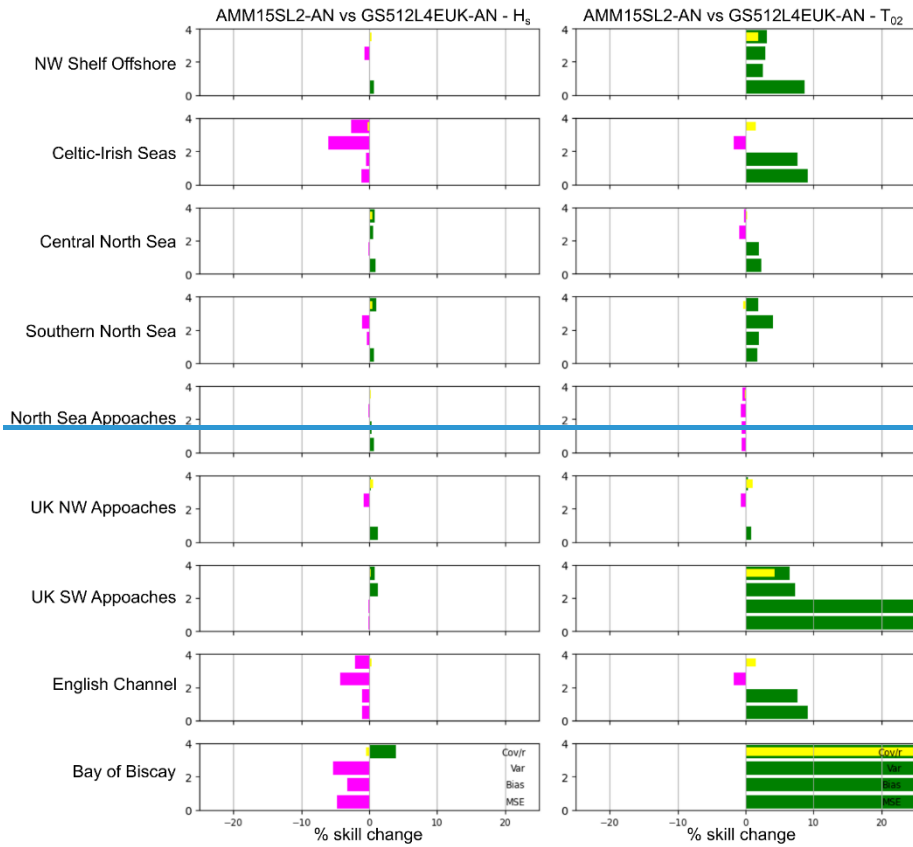
32

Figure 6. In-situ observations-model comparison and error changes of significant wave height (H_s; left panels) and mean zero up-crossing period (T_{02}; right panels) for AMM15SL2-AN versus GS512L4EUK-AN for the different areas of analysis inside the NW shelf – UK waters domain. Magenta (decrease of skill score) and green (increase of skill score) bars represent percent of skill change of AMM15SL2-AN with respect to GS512L4EUK-AN. Yellow bar indicates change in correlation. Refer to Fig. 1 for the

AMM15SL2-AN vs GS512L4EUK-AN
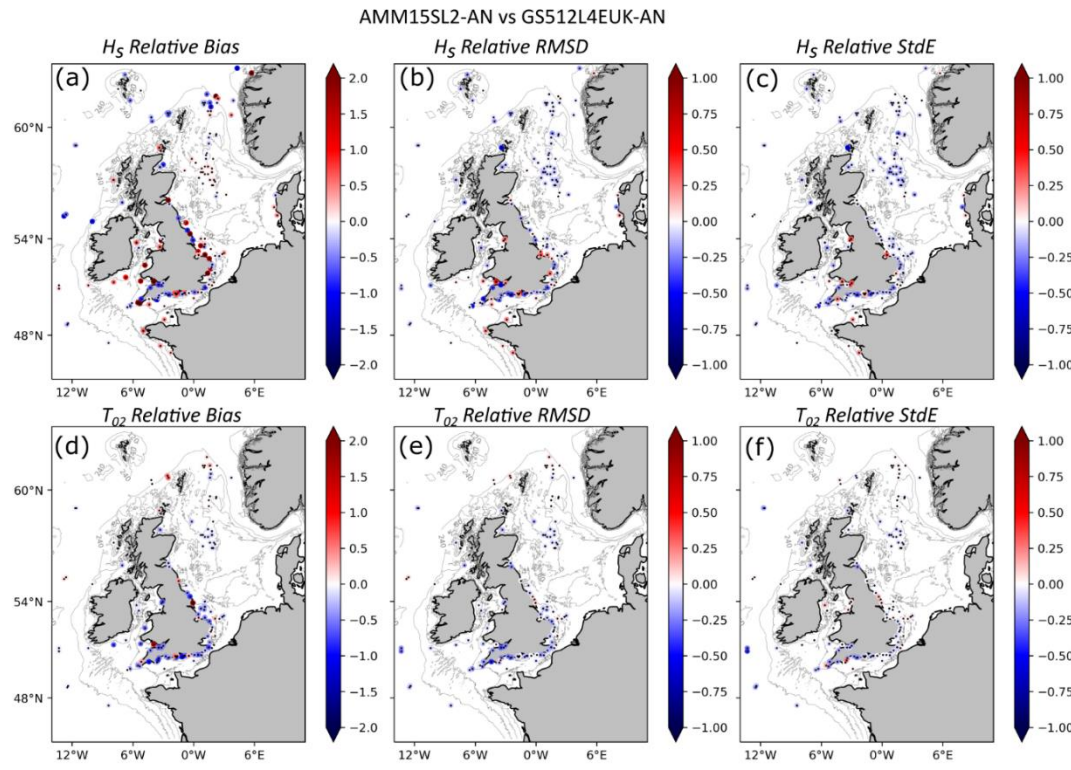
Figure 7. Relative change in absolute *bias* (a,d), *RMSD* (b,e) and *StdE* (c,f) between observations-model comparison for AMM15SL2-AN and GS512L4EUK-AN for significant wave height (H$_s$) and mean period (T$_{02}$) across UK waters. Stats are computed over 2019–2020 and observations included are JCOMM-WFVS, SHPSYN and WAVENET. Negative (positive) values indicate a reduction (increase) of the metric by AMM15SL2-AN. To facilitate visualisation when no relative change is observed, all in-situ locations are indicated with a black dot.

5.4 Wave-current interaction

The addition of surface currents has effects on wave generation, advection and refraction, with the latter being one of the main wave-current processes affecting the wave field in areas with large tidal currents such as those on the shelf. We focus now on areas where the tide has a dominant effect on the wave field using WAVENET in-situ directional wave buoys.

When comparing GS512L4EUK and AMM15SL2, we showed that wave-current interaction in areas where tidal currents are important produces larger wave heights and positive changes in the wave period and direction. An example of these fluctuations is presented at Start Bay wave buoy (Fig. 8), which is a tide modulated coastal in-situ location in the English Channel. Adding the wave-current interactions leads to a reduction of the small negative H$_s$ *bias* at this site from -0.11 to -0.02 m with a reduction of the *RMSD* from 0.2m to 0.14m. The quantile-quantile relationship (QQ) for H$_s$ at this location shows that both configurations are in very good agreement with observations (*r*=0.95 and 0.97 for GS512L4EUK-AN and AMM15SL2-AN, respectively) and both tend to underestimate the tail of the distribution; however, this is much closer to observations in AMM15SL2-AN. T$_{02}$ QQ shows an underprediction of the lower periods

34

(T_{02}=2–6s with *bias*=0.5–1s; Fig. ~~9~~8c,d) and a significant overestimation of larger periods (T_{02}>8s) that is accentuated in the regional configuration. Despite this, overall T_{02} metrics are improved when currents are accounted for~~in AMM15SL2-AN:~~ ~~bias of -0.92 to -0.70, RMSD of 1.36 to 1.22s and r of 0.56 to 0.61.~~. In line with the improvement of Dir by AMM15SL2-AN present in most coastal locations, Dir *RMSD* at Start Bay is significantly reduced from 44º to 32.25º and this is reflected in a significant reduction ~~on~~ of the model biases. ~~Hence, StdE is equivalent to approximately 27% of the SDobs at this location.~~
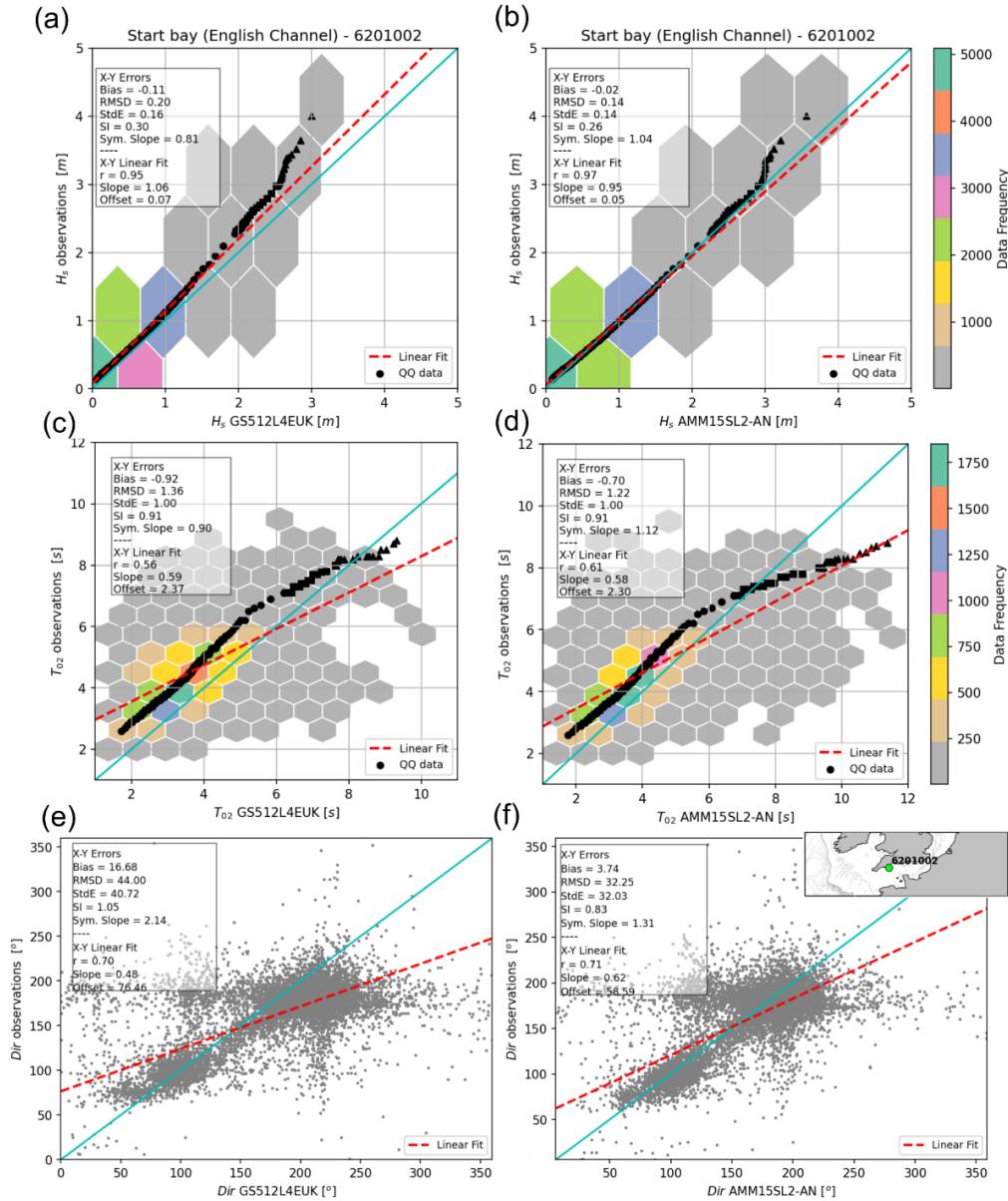
Figure ~~8~~9. (a,b) Significant wave heigh (H_s) and (c,d) mean period (T_{02}) quantile-quantile relationship and scatter data for GS512L4EUK-AN (left column) and AMM15SL2-AN (right column) at Start Bay in-situ wave buoy. (e,f) Scatter plots for wave

35

direction (Dir) at Start Bay in-situ wave buoy. Inset with wave buoy location is presented in panel (f). Wave bulk stats are included in each individual panel and correspond to the comparison between model and observations over 20190101 to 20201231.

Tidal modulation of the wave field is observed in several locations. As an example that ~~can be extrapolated to~~is representative of most coastal areas, Fig. ~~10~~9 shows the timeseries of H_s, T_{02} and Dir for both configurations at the Scarweather wave buoy, located in the Bristol Channel, where an increase in the observed T_{02} and H_s can be seen during each tidal cycle (Fig. 9a,b). This modulation is only present in the AMM15SL2 configuration; however, sometimes a lag in the tidal fluctuation (3h for Scarweather; up to 6h in other locations) ~~is presen~~occurs ~~t~~between model and observations that may lead to poorer metrics than when no currents are used (i.e. the run without currents provides a smoother signal~~similar to a filtered signal~~). In line with some additional forcing evaluation of the current field (refer to *Supplementary material*), this lag is linked to the negative veering (tidal phase) that is present in the modelled currents where observations tidal velocities lead the model velocities. ~~This lag in the tidal phase, veering, for AMM15 ocean was previously observed in Tonani et al. (2019). H_s and T_{02} present an inverse behaviour as the mean period is consistently underpredicted during all stages of the tide but this underprediction is stronger during high tide (Fig. 910b), whereas H_s is overpredicted and this positive *bias* is greater during low tide (Fig 910a). This suggests that other non-linear effects that are important in coastal locations such as triad wave interactions are (currently missing in both configurations) should be included in future system upgrades.~~ Equally, it is also noted the importance of the tidal modulation on the wave direction present in AMM15SL2-AN timeseries captured on the observations within a range of +/-30 degrees (Fig. ~~10c~~9c) in these coastal wave buoys.
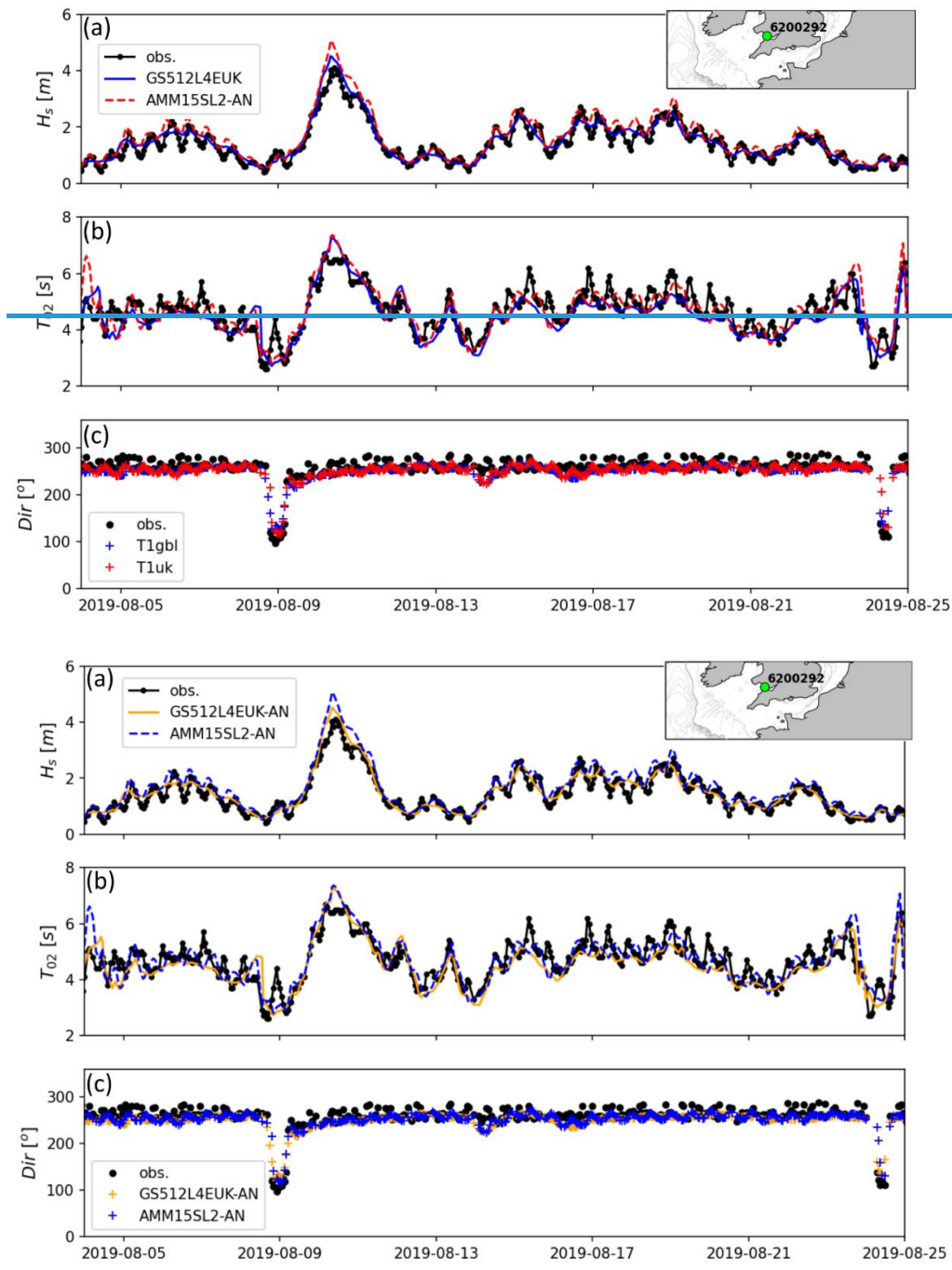
Figure 910. Timeseries of (a) significant wave heigh (H$_s$), (b) mean period (T$_{02}$) and direction (Dir) for GS512L4EUK-AN and
AMM15SL2-AN (right column) at Scarweather in-situ wave buoy. Inset with wave buoy location is presented in panel (a).

Differences in the accuracy of both ~~baseline~~ configurations suggests that wave refraction and shifts in the relative frequency
are better captured with the addition of the sea surface currents in most of the domain. However, overall metrics for H$_s$ are

slightly weaker in certain areas of analysis such as the Irish and Celtic Seas, English and Bristol Channel and E coast of England. In order tTo isolate the effect of currents and not account for any differences in resolution, we run the AMM15SL2 configuration without currents during August 2019 and compare model differences in H_s over two tidal cycles during spring tides (Fig. 10a). Positive residual differences in H_s correspond to those locations where AMM15SL2 presents some degradation respect GS512L4EUK. Model evaluation showed that both configurations GS512L4EUK and AMM15SL2 tend to slightly overestimate H_s, hereintherefore, the overall positive bias is exacerbated by the contribution of the residual currents in AMM15SL2. Additionally, the evaluation of the currents effects on the wave energy distribution in two different shallow coastal locations demonstrate that including tidal currents produces a consistent shift towards longer periods (Fig. 10e,g) reducing the energy bias between model and observations at low frequencies (not shown), hence the better agreement for the period in AMM15SL2. In terms of Dir, model differences during ebb (Fig. 10b) and flowod (Fig. 10c) tide conditions show wave refraction angles of ±10º when currents are included, helping to better capture the distribution of the wave energy in the directional space (e.g., Fig. 8f). This suggests that AMM15SL2 is capturinges the distribution of the energy in terms of frequency and direction better whereas the total energy might be sometimes too large in this configuration. In other words, the bulk energy imparted to the ocean surface waves might be excessive during low-midoderate conditions.
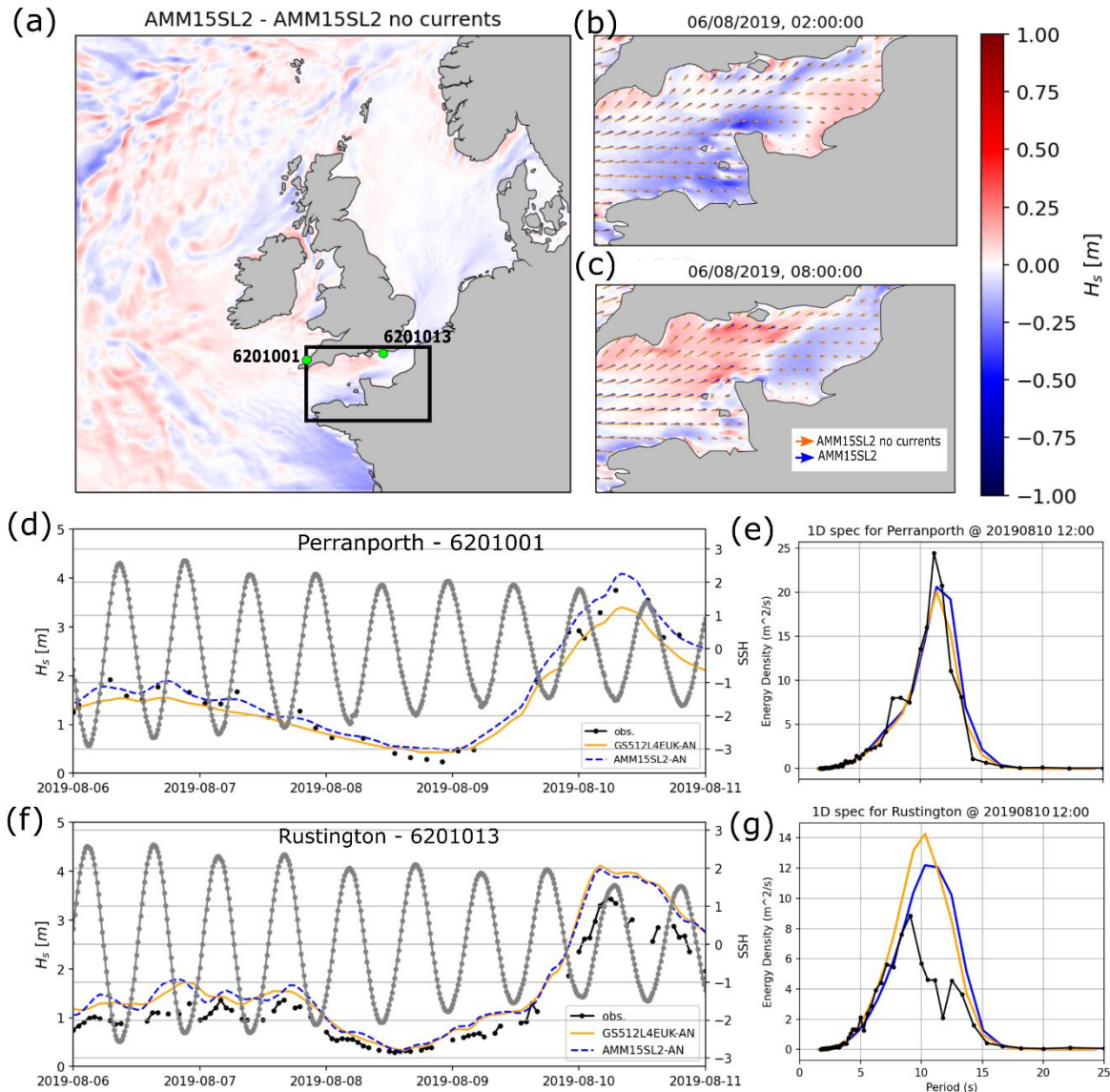
38

Figure 10. Effects of currents in significant wave height (H_s). (a) Mean difference over two tidal cycles (25h) between AMM15SL2 and GS512L4EUK for H_s (a) across UK waters. (b,c) Snapshots of H_s difference over the English Channel (see panel (a) for zoom reference) during ebb (b) and flood tide (c) conditions with vectors for wave direction. (d,f) Timeseries of sea surface height (SSH) and Hs and (e,g) 1D spectra in Perranporth (6201001) and Rustington (6201013) directional waveriders during a storm event in August 2019. Wave buoy locations are presented in panel (a).

3.5 Verification of extremes across the NW shelf - UK waters

Wave models tend to struggle to replicate storm events as uncertainty in both storm evolution in the atmospheric forcing and source term parameterisations is high (Valiente et al., 2021a). Model performance is evaluated for the period of *only storm*, using those observations and model GS512L4EUK-AN and AMM15SL2-AN data exceeding the 90th percentile. In this case

we define a storm period when $H_s > H_{s,90\%}$ (Q90). Three major features are repeated in the system performance when reproducing the extremes: (i) both configurations tend to overpredict H_s in the sheltered coastal locations and slightly underpredict in other areas of analysis; (ii) T_{02} tends to be underestimated in most of the domain; and (iii) model errors reproducing the wave diagnostics are larger in the SW area of the domain and along very sheltered coastal locations.

There is a tendency to underestimate extremes in most areas of analysis with some exceptions: coastal locations in the E of English Channel and Bay of Biscay. These coincide with locations where T_{02} is also overestimated. Refer to Fig. 10 where the timeseries show how AMM15SL2-AN picks up the peak of the waves and represents the tidal modulation; although sometimes this is translated to larger biases than GS512L4EUK-AN during storms. In other words, the feature of the wave field evolution may be represented in the model but not always at the exact time in sheltered coastal locations. Equally, during stormy episodes the peak of the wave field is exacerbated with the inclusion of the currents in most coastal locations, sometimes leading to larger overestimation rates than GS512L4EUK configuration; hence, the degradation in *bias* by AMM15SL2 configuration. Conversely, H_s *RMSD* values are reduced in AMM15SL2-AN (i.e., negative relative *RMSD*).
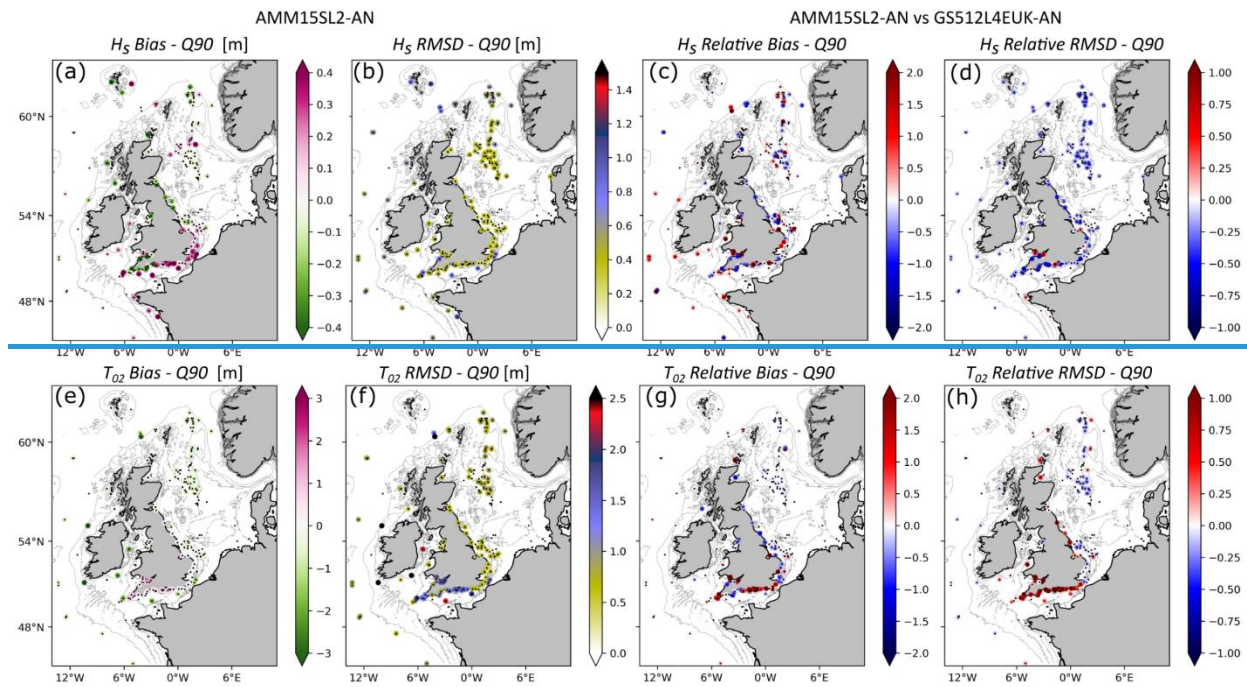

Figure 11. Observations-model comparison and relative change for the quantile of 90% (Q90) for significant wave height (H_s) and mean period (T_{02}) in AMM15SL2-AN across UK waters. (a,e) *Bias* and (b,f) root mean square error (*RMSD*) between modelled H_s and T_{02} and in-situ observations; and relative change in (c,g) absolute bias and (d,h) RMSD between observations-model comparison for AMM15SL2-AN and GS512L4EUK-AN. Stats are computed over 2019-2020 and observations included are JCOMM-WFVS, SHPSYN and WAVENET. Negative (positive) values indicate a reduction (increase) of the metric by AMM15SL2-AN. To facilitate visualisation when no relative change is observed, all in-situ locations are indicated with a black dot.

It should be highlighted that latest model developments improved the system performance during mid to high energy (i.e., extremes) conditions that lead to a significant improvement on the Q90 statistics across the North Sea. Equally, this

improvement in representing the extremes was also observed across the coastal locations, mainly for the quantile of the 99% (not shown). Model skill improvement representing the extremes was achieved with the combination of a reduction of the sheltering for short waves (TAUWSHELTER term) and a bulk adjustment to the wind field through a decrease of the maximum value allowed for wind-wave coupling (BETAMAX term).

53.65 Impact of resolution on wave growth

Increased resolution has been demonstrated to play an important role in model skill score. However, the advantages on of using higher spatial resolution in AMM15SL2 (Fig. 11) do not always show in the overall skills of H_s. We It is known that model simulations can show significant sensitivity to spatial resolution and source term model set-up. All configurations in the Met Office wave forecast system include the same source term tuning parameters (refer to *Supplementary material*) as this has been found to be suitable in previous system versions. In order tTo test the sensitivity to of spatial resolution, we run a number of WW3 idealised numerical experiments with variable resolution. The domain has an extentsion of 1000km x 500km that is discretised with regular grids of 10km, 5km and 2.5km resolution; experiments 10kmRes, 5kmRes and 2.5kmRes, respectively. All resolutions are then explored for deep water (flat bathymetry of 1000m depth) and shallow water (flat bathymetry of 40m deep) conditions. The model is forced for 48h by a constant wind speed ranging from 10 to 30ms^{-1}. All simulations include the same source term configuration and tuning terms.
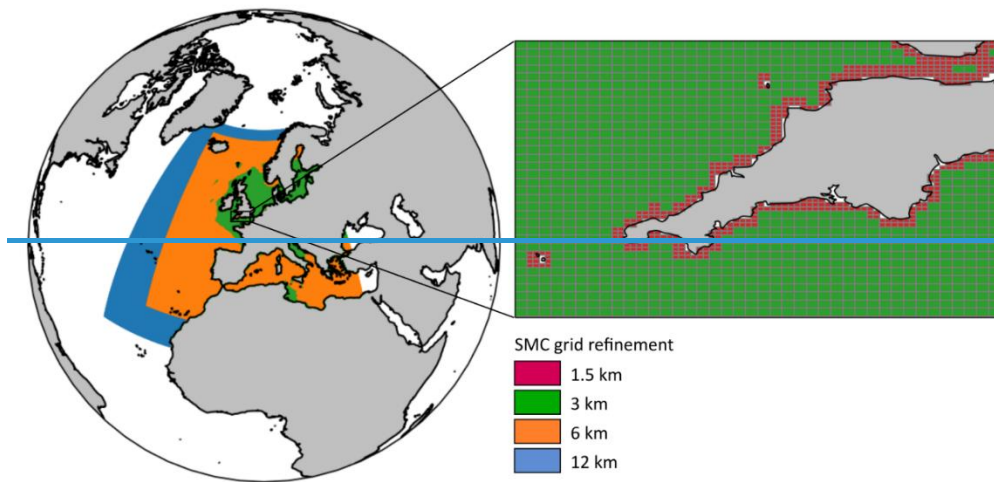

SMC grid refinement
- 1.5 km
- 3 km
- 6 km
- 12 km

Figure 811. GS512L4EUK Spherical Multiple Cell grid refinement (left; highest resolution is 3km) with zoom in the Southwest of England (right; coastal cells resolution is 1.5km) showing coastal waters refinement as resolved in AMM15SL2.

Dimensionless fetch limited growth (gH_s/U_{10}^2) curves as a function of dimensionless fetch ($gfetch/U_{10}^2$) for the different idealised experiments are presented in Fig. 121. For reference, the theoretical wave growth relationships derived from observations by Young and Verhagen (YV96; Young and Verhagen, 1996 Young and Verhagen, 1996) is are also included.

41

805 The difference in wave growth between resolutions is greater for shorter fetches and lower winds. High resolution ~~simulations~~ ~~waves~~ grids (i.e., 2.5kmRes) generate higher waves compared to YV96 relationship for both deep (Fig. ~~12a~~11a,c,e) and shallow (Fig. ~~12b~~11b,d,f) water. This behaviour for short fetches is consistent for all wind speeds with higher resolution resulting in larger growth rates. In all cases ~~and~~ differences between resolutions become smaller ~~for stronger winds~~as wind speed increases. ~~Furthermore, higher resolution presents larger growth rates for shorter fetches and growth differences for the different~~ 810 ~~resolutions decrease with the wind speed.~~ Idealised experiments suggest that the increased resolution in AMM15SL2-AN might lead to faster wave growth and subsequently larger H_s for mid to high-energy wind conditions in fetch-limited areas. Accordingly, model-observation results show that for modal conditions, although both models ~~AMM15SL2-AN t~~tends to slightly overestimate H_s, neutral or some skill weakening reproducing H_s is observed in AMM15SL2-AN ~~and this is better~~ ~~replicated by GS512L4EUK-AN~~. Conversely, extremes, although generally underestimated (not shown), tend to be better 815 replicated by AMM15SL2-AN mainly in fetch limited locations (e.g. at Start Bay; Fig. 8a,b). ~~-~~The implication is that ~~in order~~ to obtain a similar behaviour in all model configurations, the next generation of Met Office modelling systems should include a modified parameterization that is domain dependent as the current source term set-up is more optimised for GS512L4EUK configuration and modal conditions.
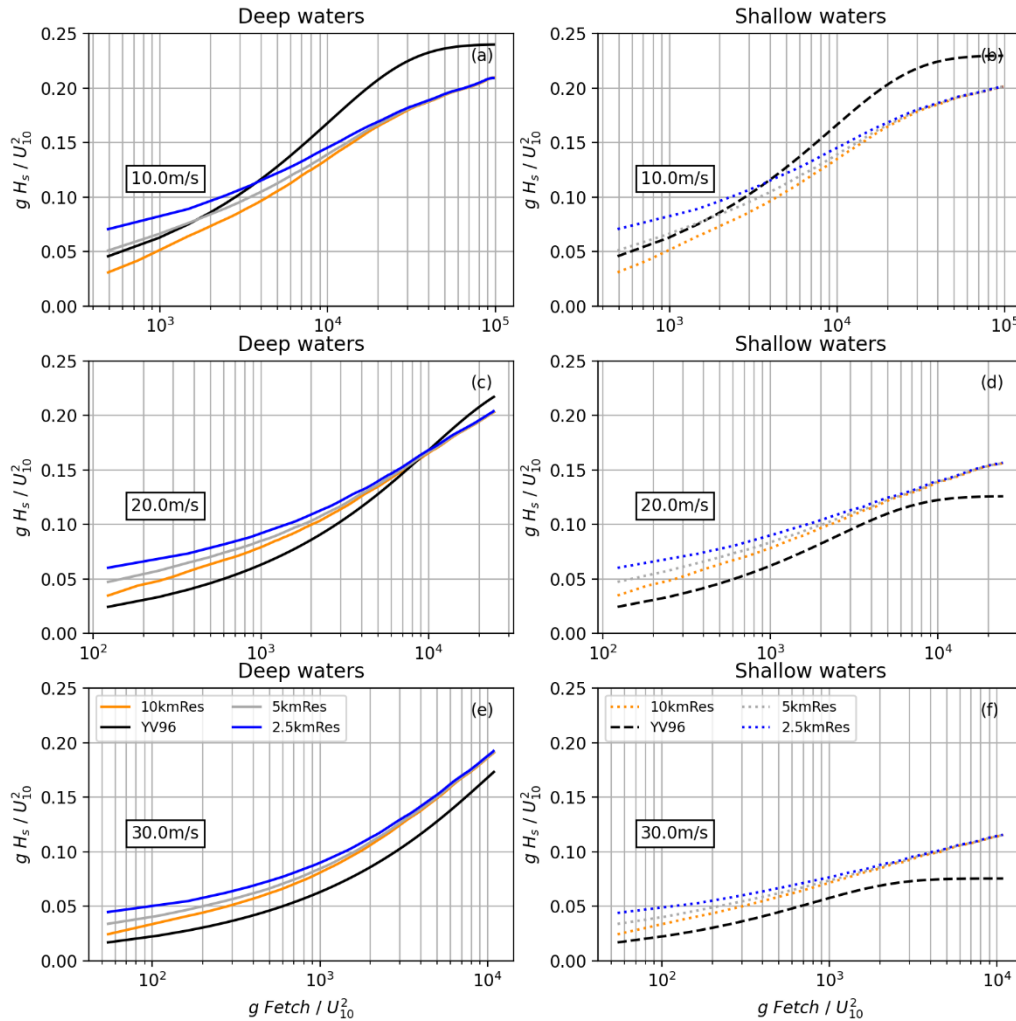
Figure 112. Dimensionless wave growth curves for different model grid resolutions (10km, 5km and 2.5km) as a function of dimensionless fetch. Fetch limited growth curves are computed for (a,c,e) deep water and (b,d,f) shallow water (40m depth) for constant winds of 10, 20 and 30ms^{-1}. The theoretical curve of Young and Verhagen (1996) is presented (YV96). Results for the different configurations correspond to 48h model runs.

4 Forecast performance

Forecast wave system performance for the two baseline configurations was evaluated during 50 days in summer (from 20190619 to 20190814; JJA) and winter (20191204 to 20200124; DJ) across the NW shelf – UK waters. These shorter experiments replicate the latest operational configuration using both the most up to date wave model version (i.e., WAVEWATCH III® at version 7.12) and the most up to date NWP winds (as described in *Sect. 2.4*). FCST experiments used the corresponding T+6 restart output file generated in the analysis runs for initialisation of each trial. All FCST runs cycled every 6-hours with the 00Z cycle on each day triggering a 144-h forecast. Hence, updated winds were used for the first six

43

hours of each cycle adding the forecast winds after the first six hours of 00Z cycle. Refer to *Sect. 2.4* and Table 1 for more information on the temporal and spatial resolution of the forcing conditions. For comparison purposes, AMM15SL2 FCST runs was up to T+144 as per GS512L4EUK FCST, as opposed to T+66 used in operations. It is noted that currents as forcing were lacking in the last 78 hours of the AMM15SL2 FCST runs.

Table 5 Experiments specifications for forecast capability.

Experiment	Description
GS512L4EUK FCST	JJA (20190619 to 20190814) and DJ (20191204 to 20200124) forecast run global. Forcing: forecast 10km NWP winds and updated fraction of sea ice. Restart at T+6 T+144 forecast at 00Z cycle
AMM15SL2 FCST	JJA (20190619 to 20190814) and DJ (20191204 to 20200124) forecast. Forcing: forecast 10km NWP winds and AMM15 FOAM analysis and forecast currents. Restart at T+6 T+144 forecast at 00Z cycle

Fig. 13 shows bias and RMSD for wind forcing conditions over the summer months of JJA and the winter months of DJ. Forecast evaluation encompasses from T+24 hours to T+144 hours. Winds tend to be overestimated in both configurations during most of the forecasting period up to T+96. Further inside the forecast lead time, winds appear to be slower versus the first forecast days, and the tendency is to show a reduced *bias* that might be also associated with cancellation errors (Fig. 13a,b). This overall wind speed decrease is more accentuated over the winter months (DJ) in both systems. GS512SL4EUK and AMM15SL2 *biases* are almost constant around 0.4–0.6 and 0.1–0.3 ms^{-1}, respectively up to T+96, decreasing to 0.1 and 0.2 respectively at the end of the forecast. U_{10} *RMSD* oscillates 1.5–2.5ms^{-1} up to T+96 and increases to 3.5ms^{-1} in the last two days of forecast. *RMSD* for U_{10} dir is almost equal for the two systems during both winter and summer months with values oscillating from 20º at T+24 up to 60º at T+144 (Fig. 13g,h). This indicates that the errors between model and observations are steady in space and increase in time.
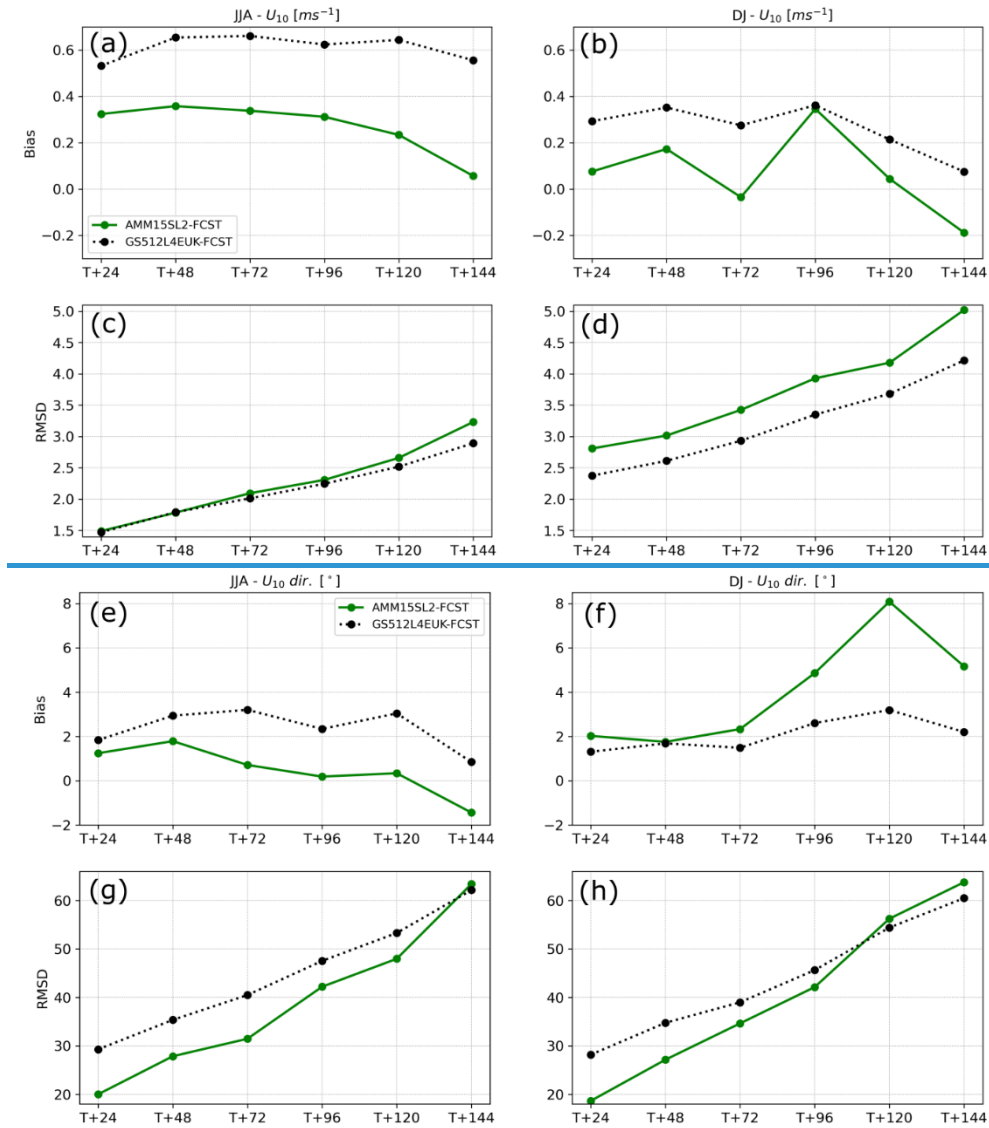
45

with >20% reduction in *RMSD* compared to the global configuration for T_{02}, due to better representation of bathymetric features, depth related processes and wave current interaction (Fig. 14e-h). Metrics seasonality for both H_s and T_{02} bulk parameters is also observed in all the leading times with larger values of *RMSD* during DJ.
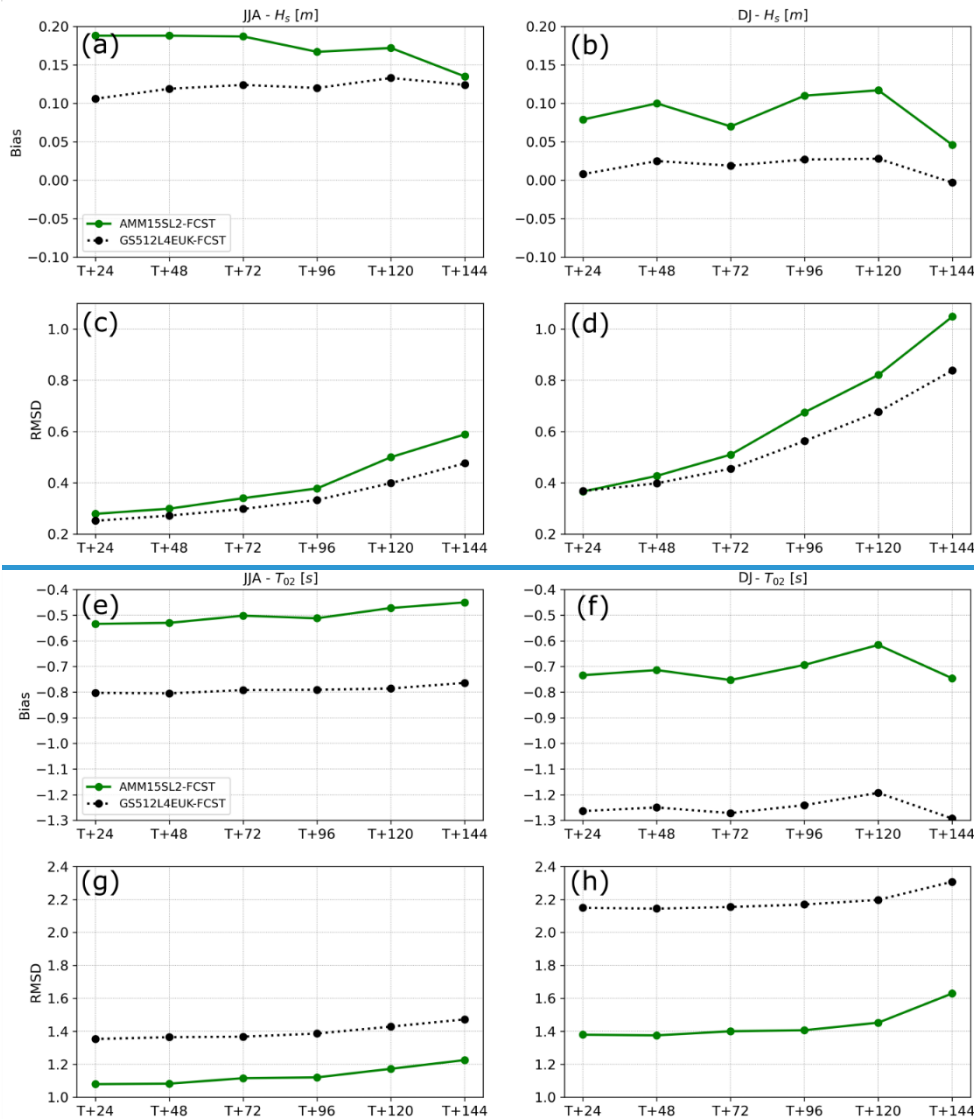
Figure 14. Forecast (a,b,e,f) *bias* and (c,d,g,h) root mean square error (*RMSD*) for significant wave height (H_s) and mean period (T_{02}) every 24 hours over a forecast period of 6 days (T+144). Values are averaged over the months June-July-August (JJA; left panels) and December-January (DJ; right panels) and correspond to the UK waters model (AMM15SL2-FCST; solid line) and the global model (GS512L4EUK-FCST; dashed line).

As expected, the forecast skill of both configurations decreases steadily with lead time (i.e., positive trend) for both forcing and wave bulk parameters (i.e., U_{10}, H_s and T_{02}). This decrease in the forecast skill appears to be relatively steady for the first four days of forecast (up to T+96); however, *RMSD* trend indicates a more rapid decrease in the forecast skill after these. It is

46

~~noted that the degree of decrease in the forecast skill for the case of T_{02} is smaller comparing with H_s and in fact, values of *bias* (-0.8s and -0.5s for GS512SL4EUK FCST and AMM15SL2 FCST during JJA, respectively) and *RMSD* (1.4s and 1.1s for GS512SL4EUK FCST and AMM15SL2 FCST during JJA, respectively) are almost constant for the first four days in both JJA (Fig. 14e,g) and DJ (Fig. 14f,h) periods.~~

6~~5~~ Discussion and ongoing development~~Summary and future developments~~

We ~~In sections 4 and 5 we~~ have presented a comprehensive evaluation of two of the Met Office operational wave configurations: the global ~~standalone determinist~~ GS512L4EUK and the regional ~~standalone deterministic~~ AMM15SL2. Both models show good performance when compared to different observation datasets and this skill is retained for all lead times in the forecast~~, with a degradation in performance that is mostly attributed to the wind forcing~~. We have illustrated the benefits of the SMC grid, that allows to resolve the propagation in open waters at lower resolution and to incorporate the effect of complex bathymetry and coastline as waves approach to shore. ~~In addition, we have~~We put particular attention in studying two relevant aspects that describe the benefits provided by AMM15SL2: the impact of incorporating currents ~~to model tidal effects~~ and the implications of higher resolutions in wave growth~~, which we discuss in more detail in the following paragraphs.~~~~The latest developments and performance of the current Met Office operational wave system have been presented. Performance of the system was focused on the global (GS512L4EUK) and the NW shelf - UK waters (AMM15SL2) baseline configurations. The evaluation of system performance and forecast capability shows a good agreement with both satellite and in situ observations and demonstrates the quality and accuracy of the Met Office wave forecast capability. As expected, forecast skill decreases steadily with lead time for both forcing and wave parameters; however, this decrease is slower up to T+96. Model-observations correlation is beyond 0.94-0.96 in all areas of analysis with standard deviations of differences that correspond to maximum 13-25% of the observed mean bulk wave diagnostics. The inclusion of wave-current interaction and the higher resolution for depths <40m in AMM15SL2 together with a better representation of the local features (e.g., headlands, highly spatially variable bathymetry) help to significantly improve the prediction of the wave direction near the coast within a range of +/-30 degrees and the mean period with >20% reduction in the RMSD. This is also a consequence of the increase in wind forcing resolution (10km). Winds in AMM15SL2 are not up-scaled in the pre-processing routine as it is performed in GS512L4EUK (i.e., 10km resolution winds interpolated to a 25km regular grid). H_s is better forecasted overall on the GS512L4EUK, which we attribute to an energetic tunning of the source term yielding in an overestimation on AMM15SL2; consequently, extremes are better forecasted on the AMM15SL2. This improved skill, together with a better prediction of mean upcrossing period and wave direction, has large implications for the prediction of waves approaching coastal locations and subsequently in beach safety, risk to flooding and overtopping and shoreline evolution in general. It is also recognised that despite a good skill of AMM15SL2 replicating inshore waves, the model utility in coastal zones largely sheltered and/or with strong shallower water bathymetric variability should be treated with caution as there are important non-linear effects that are not included in any of the baseline configurations.~~

900

Recent studies have demonstrated positive impacts on significant wave height prediction when surface ocean currents are accounted for (e.g., ., Palmer and Saulter, 2016; Ardhuin et al., 2017; Echevarria et al., 2021; Valiente et al., 2021b) Hersbach and Bidlot, 2008; Palmer and Saulter, 2016; Ardhuin et al., 2017; ; b). AMM15SL2 based configuration includes wind and sea surface currents as forcing conditions. Accurate representation of the wave-current interactions across the NW shelf - UK

905 waters domain is essential as ocean-wave coupling improves accuracy of the ocean surface dynamics by 4% (Bruciaferri et al., 2021). Additionally, it is clear that the presence of currents can modify the distribution of the wind waves on the shelf with >15% impact during modal conditions (e.g., Ardhuin et al., 2017; Valiente et al. , 2021b; Alday et al., 2022) Ardhuin et al., 2012; Valiente et al. , 2021b; Alday et al., 2022). Although relative changes in T_{02} metrics and wave Dir show an overall significant improvement (>25% in *RMSD* and 10% in *bias*), tThe quantitative assessment to demonstrate the improvement of

910 the forecast skills in the significant wave height diagnostic by AMM15SL2 with respect to GS512L4EUK has been provesd difficult in some instances. AThe lag between model and observations is present in some in-situ locations due to the tidal modulation (i.e., larger spread on the observation-model differences and possible double penalty effect; Crocker et al., 2020), together with an excessive bulk energy imparted to the ocean surface waves in AMM15SL2 configuration (consequence of the numerical choice), that leads sometimes to poorer metrics than when no currents and higher resolution are used (i.e.,

915 GS512L4EUK).

This is related to a lag between the model and observations and a potential double penalty effect in the verification as a result, as well as possible cancellation errors in GS12L4EUK-AN. Previous studies demonstrated that metrics based on direct point matchup between model data and observations might often lead to the double penalty effect (Crocker et al., 2020), where features are correctly predicted but misplaced with respect to the observations.

920 Although relative changes in T_{02} metrics and wave Dir show an overall significant improvement (>25% in *RMSD* and 10% in *bias*) of these diagnostics when currents and higher resolution are introduced, a larger spread on the observation model differences for H_s is also observed. This is considered to be linked to the double penalty effect (Crocker et al., 2020), where features are well predicted but misplaced with respect to the observations. Discretization and numerical schemes (e.g., Roland and Ardhuin, 2014), together with forcing accuracy and the choice of the parameterisation for wave growth and dissipation

925 (e.g., Ardhuin et al., 2010; Zieger et al., 2015) are among the main factors affecting the accuracy of a spectral model (e.g., Alday et al., 2022). In this lineIn our evaluation, we show that resolution and the choice of the numerical tuning significantly influences the model accuracy. Furthermore, model skill improvement representing modal/ extreme conditions can be optimised but often leads to degradation of part of the distribution of the wave field. Met Office latest configuration changes from ST4 source term defaults included a combination of a reduction of the sheltering for short waves (TAUWSHELTER

930 term) and a bulk adjustment to the wind field through a decrease of the maximum value allowed for wind-wave coupling (BETAMAX term), leading to an increase in model accuracy reproducing the tail of the distribution that subsequently led to some degradation in those sectors where the model was already overestimating.

The latest developments and performance of the current Met Office operational wave system has been presented.

Imminent system developments will includeincorporate:

- (i) the Uuse of sea point wind forcing in the SMC grid, improving the wind transfer between atmosphere and ocean. The change in the pre-processing of the wind forcing conditions task will include sea point winds (i.e., SMC grids cells) instead of the current pre-processing step where winds are interpolated to the underlaying grid resolution (25km for GS512L4EUK and 3km for AMM15SL2) in which 10km NWP Met Office wind resolution for the global domain is up-scaled. This development will help correcting some of the wave model behaviour in certain areas of the globe where an improvement in wind speed and direction due to the higher resolution interpolation is likely to be an important factor.; and (ii)

- Othe optimisation of the models in line with model resolution. The change in the pre-processing of the wind forcing conditions task will include sea point winds (i.e., SMC grids cells) instead of the current pre-processing step where winds are interpolated to the underlaying grid resolution (25km for GS512L4EUK and 3km for AMM15SL2) in which 10km NWP Met Office wind resolution for the global domain is up-scaled. This development will help correcting some of the wave model behaviour in certain areas of the globe where an improvement in wind speed and direction due to the higher resolution interpolation is likely to be an important factor. Additionally, iIdealised scenarios showed resolution dependent wave growth indicating that it is important to optimise the source term parameterisation for the different spatial resolutions. Model-observation errors observed in AMM15SL2 for modal conditions are expected to be reduced after the retuning of the regional model to better match observations across the coastal UK waters as currently this is more optimised to better capture extremes and for the global model.

- SMC multigrid. Implementation of a multigrid approach for the global domain that will allow for improved scaling and a hybrid parallelisation (component and domain decomposition) in hybrid MPI-OpenMP mode.

Long term improvements in the Met Office operational wave forecasting system will focus on various areas which include improving computational efficiency with the use of the SMC multigrid and exploring data assimilation. The Met Office has recently demonstrated the benefits of running SMC in multigrid mode (Li, 2022) and the next development steps will be to work towards implementing a multigrid approach for the global domain that will allow for a hybrid parallelisation (component and domain decomposition) in hybrid MPI-OpenMP mode. This improvement was tested and results show large reductions in computational time and memory demand, permitting future model updates with increasing resolution (Li, 2022) and a more efficient use of high performance computers based on GPUs. Additionally, various studies have shown benefits from using data assimilation to improve the wave initialisation (Saulter et al., 2020a, Aouf et al., 2021). Previous attempts using AMM15SL2 configuration demonstrated a small positive impact of the assimilation scheme on H$_s$ forecast skill over lead times of up to 12h. In future years we will explore the benefits of using data assimilation in our operational systems.

Future systems will include the waves as a system component of a more comprehensive atmosphere-wave-ocean-land-ice system. Met Office research is also focused on delivering more accurate and comprehensive forecasts of the wider earth system (Graham et al., 2018; Tonani et al., 2019). This implies, in most cases, a need to develop more integrated systems where the different physical components (i.e., atmosphere, ocean, ice and waves) are coupled (e.g., Lewis et al., 2019; Bruciaferri et al.,

2021; Valiente et al., 2021a; Castillo et al., 2022). ~~(e.g., Lewis et al., 2019; Bruciaferri et al., 2021; Valiente et al., 2021a; Castillo et al., 2022).~~ In recent years, the Met Office has put significant effort into the development of fully coupled ~~(atmosphere, wave, ocean and sea-ice) global and regional~~ models and although an operational AMM15 ocean-wave coupled system has been ~~released~~deployed, ~~other~~ more complex atmosphere-wave-ocean coupled ~~systems~~models ~~are still far from becoming~~are currently in a pre-operational research phase. The GS512L4EUK wave model described in this paper is in the process of being implemented in a global research atmosphere-ocean-ice-wave coupled configuration; however, it will need time before it becomes operational. For the case of the operational AMM15 ocean-wave coupled with data assimilation, this is currently run once a day providing 5 days forecast. This is still computationally expensive with increased resource demands over the wave-only operational model with currents as forcing that delivers data four times a day. ~~While studies continue toward a fully coupled prediction system with atmosphere, ocean, land, ice and wave components, the maintenance and development of each of the model components is crucial in NWP. Additionally, these coupled systems are often more complex and computationally expensive with increased resource demands over a traditional standalone model.~~ Met Office internal testing demonstrates that a coupled simulation increases 10% the running time per model respect their standalone version; i.e., if an ocean model needs *n* nodes to run and a wave model needs *m* nodes, the ocean-wave coupled simulation of the two will need *n+m* nodes with an increase of 20% in the running time. While studies continue toward a fully coupled prediction system with atmosphere, ocean, land, ice and wave components, the maintenance and development of each of the model components is crucial in NWP.

7 Conclusions

The latest developments and performance of the current Met Office operational wave model forecasting system, ~~with~~focused on the global (GS512L4EUK) and the NW shelf - UK waters (AMM15SL2) baseline configurations have been presented. Model-observations correlation is beyond 0.94–0.96 in all areas of analysis with standard deviations of differences that correspond to maximum 13–25% of the observed mean bulk wave diagnostics, demonstrating the quality and accuracy of the Met Office wave forecast capability. This showcases the benefits of the SMC grid, a Met Office development, which provides computational efficiency while retaining good performance when compared to observations at both global scale and near shore. Met Office configurations are optimised to accurately predict modal conditions with a tendency to slightly overestimate. We show that tidal currents produce a residual signal that presents a more realistic looking wave time-series but can affect the final accuracy of the model. Th~~is~~at is, areas where the tidal currents increase (decrease) the significant wave height led to some degradation (improvement) of this parameter by AMM15SL2.

The inclusion of wave-current effects and the higher resolution for depths <40m in AMM15SL2 together with a better representation of the local features (e.g., headlands, highly spatially variable bathymetry) result in an incremental improvement in the representation of the wave field mainly in the frequency and directional domain. The prediction of the wave direction

near the coast is improved within a range of +/-30 degrees and the mean period shows >20% reduction in the RMSD with respect to GS512L4EUK. This is also a consequence of the increase in wind forcing resolution (10km), as winds in AMM15SL2 are not presently up-scaled in the pre-processing routine ~~as it is~~ performed ~~in~~for GS512L4EUK (i.e., 10km resolution winds are interpolated to a 25km regular grid).

We demonstrate that resolution and the choice of the numerical tuning significantly influences the model accuracy. Evidence of resolution dependent differences in wave growth was observed, leading to slightly overestimated significant wave heights when replicating coastal mid-range conditions by AMM15SL2. This is ~~, and~~ better suited to replicate the extremes, particularly on regions with short and mid fetches such as the North Sea. ~~.~~

The improved skill of AMM15SL2, together with a better prediction of mean upcrossing period and wave direction, has large implications for the prediction of waves in shot fetched areas and ~~approaching~~ coastal locations. This provides benefits for both off-shore infrastructures, such as wind power or oil platforms, as well as in coastal applications like ~~and subsequently in~~ beach safety, risk to flooding and overtopping and shoreline evolution in general.~~.~~ It is also recognised that, despite a good skill of AMM15SL2 in replicating inshore waves, the model utility in coastal zones largely sheltered and/or with strong shallower water bathymetric variability should be treated with caution as there are important non-linear effects that are not included in any of the baseline configurations.

Data availability. The length, resolution and spatial coverage of the data generated in running the trials described in this paper requires a large storage facility. The complete or partial data will be available via request to the corresponding author. Data used for the model evaluation and analysis in this paper in the form of model-observations match-up netCDF files are available via https://doi.org/10.5281/zenodo.7019826.

Datasets for model evaluation include different sources. SHPSYN in-situ observations is accessed via the Global Telecommunication System but it is also publicly available via http://www.marineinsitu.eu/dashboard/. WAVENET in-situ data is obtained from the National Network of Regional Coastal Monitoring Programmes and CEFAS Wavenet, and should be available prior registration at http://www.channelcoast.org/~~-~~ and https://www.cefas.co.uk/cefas-data-hub/wavenet/. JCOMM-WFVS observations are obtained as Met Office is part of the World Meteorological Organisation - International Oceanographic Commission (WMO-IOC) Joint Commission On Marine Meteorology's operational Wave Forecast Verification Scheme. MA_SUP03 satellite altimeter data is available for public download and can be obtained prior registration via FTP in ftp://ftp.ifremer.fr/ifremer/cersat/products/swath/altimeters/waves/data~~.~~.~~-~~

Additional information on the data acquisition of the different observational datasets used in this paper is included in the ~~Supplement~~Supplementary material.

Code availability - Obtaining WAVEWATCH III®. The version of WAVEWATCH III used operationally at the Met Office is publicly available via the Met Office's "Trusted Institutional Fork" of the NOAA WW3 GitHub repository:

https://github.com/ukmo-waves/WW3/tree/ukmo_ps45-1.hotfixes. The WAVEWATCH III code base is distributed by NOAA under an open-source style licence via http://polar.ncep.noaa.gov/waves/wavewatch/wavewatch.shtml (NOAA, 2021a). Interested readers wishing to access the code are requested to register to obtain a license via http://polar.ncep.noaa.gov/waves/wavewatch/license.shtml (NOAA, 2021b). Refer to ~~Supplement~~Supplementary material for more details.

Code availability - Obtaining configuration files. Basics of the system configuration including grid, modules and tuning parameters files are publicly available via https://doi.org/10.5281/zenodo.7148687.

Author contributions. N. G. V. conceptualised the experiments, set-up and run baseline trials, conducted the formal analysis and wind and wave verification as well as data curation, wrote the original draft and prepared figures/visualization; A. S. and B. G. helped with conceptualisation, validation resources and review and editing of draft; C. B. and J. L. contributed to model description and provided a figure for SMC visualisation; C. P. performed AMM15 currents validation; C. B., A. S., J. L., N. G. V. and T. P. contributed to the development of the wave operational system. All the co-authors contributed to the edition of the final version of the manuscript.

Competing interest. The authors declare that they have no conflict of interest.

References

Alday, M., Ardhuin, F., Dodet, G., and Accensi, M.: Accuracy of numerical wave model results : Application to the Atlantic coasts of Europe, Ocean Science, 18(6), 1665-1689, https://doi.org/10.5194/os-18-1665-2022, 2022.

Ardhuin, F., Gille, S. T., Menemenlis, D., Rocha, C. B., Rascle, N., Chapron, B., Gula, J., and Molemaker, J.: Small-scale open ocean currents have large effects on wind wave heights, Journal of Geophysical Research: Oceans, 122(6), 4500–4517, https://doi.org/10.1002/2016JC012413, 2017.

Ardhuin, F., Rogers, E., Babanin, A., Filipot, J.-F., Magne, R., Roland, A., Queffelou, P., Lefevre, J. M., Aouf, L., Babanin, A., and Collard, F.: Semi-empirical dissipation source functions for wind-wave models: part {I}, definition, calibration and validation, J. Phys. Oceanogr., 40(9), 1917–1941, 2010.

Ardhuin, F., Roland, A., Dumas, F., Bennis, A.-C., Sentchev, A., Forget, P., Wolf, J., Girard, F., Osuna, P., and Benoit, M.: Numerical Wave Modeling in Conditions with Strong Currents: Dissipation, Refraction, and Relative Wind, Journal of Physical Oceanography, 42(12), 2101–2120, https://doi.org/10.1175/JPO-D-11-0220.1, 2012.

Battjes, J. A., and Janssen, P.: Energy loss and set-up due to breaking of random waves, Coastal Engineering, 569–587, https://doi.org/10.9753/icce.v16, 1978.

Bidlot, J., Wittmann, P., Fauchon, M., Chen, H., Lefèvre, J. M., Bruns, T., Greensdale, T., Ardhuin, F., Kohno, N., and Park,

1065   S.: Inter-comparison of operational wave forecasting systems, 10th International Workshop on Wave Hindcasting and Forecasting and Coastal Hazard Symposium, North Shore, Oahu, Hawaii, 1–22, 2007.

Booij, N., and Holthuijsen, L. H.: Propagation of ocean waves in discrete spectral wave models, Journal of Computational Physics, 68(2), 307–326, https://doi.org/10.1016/0021-9991(87)90060-X, 1987.

Brown, A., Milton, S., Cullen, M., Golding, B., Mitchell, J., and Shelly, A.: Unified modeling and prediction of weather and
1070   climate: A 25-year journey, Bulletin of the American Meteorological Society, 93(12), 1865–1877, https://doi.org/10.1175/BAMS-D-12-00018.1, 2012.

Bruciaferri, D., Tonani, M., Lewis, H. W., Siddorn, J. R., Saulter, A., Castillo Sanchez, J. M., Valiente, N. G., Conley, D., Sykes, P., Ascione, I., and McConnell, N.: The Impact of Ocean-Wave Coupling on the Upper Ocean Circulation During Storm Events, Journal of Geophysical Research: Oceans, 126(6), https://doi.org/10.1029/2021JC017343, 2021.

1075   Bunney, C., and Saulter, A.: An ensemble forecast system for prediction of Atlantic-UK wind waves, Ocean Modelling, 96, 103–116, https://doi.org/10.1016/j.ocemod.2015.07.005, 2015.

Castillo, J. M., Lewis, H. W., Mishra, A., Mitra, A., Polton, J., Brereton, A., Saulter, A., Arnold, A., Berthou, S., Clark, D., Crook, J., Das, A., Edwards, J., Feng, X., Gupta, A., Joseph, S., Klingaman, N., Momin, I., Pequignet, C., Sanchez, C., Saxby, J., and Valdivieso da Costa, M.: The Regional Coupled Suite (RCS-IND1): application of a flexible regional coupled modelling
1080   framework to the Indian region at kilometre scale, Geosci. Model Dev., 15, 4193–4223, https://doi.org/10.5194/gmd-15-4193-2022, 2022.

Cavaleri, L., and Rizzoli, P. M.: Wind Wave Prediction in Shallow Water: Theory and Applications, Journal of Geophysical Research, 86(C11), 10,961-10,973, https://doi.org/10.1029/JC086iC11p10961, 1981.

Crocker, R., Maksymczuk, J., Mittermaier, M., Tonani, M., and Pequignet, C.: An approach to the verification of high-
1085   resolution ocean models using spatial methods, Ocean Science, 16(4), 831–845, https://doi.org/10.5194/os-16-831-2020, 2020.

Echevarria, E. R., Hemer, M. A., and Holbrook, N. J.: Global implications of surface current modulation of the wind-wave field, Ocean Modelling, 161(March 2020), 101792, https://doi.org/10.1016/j.ocemod.2021.101792, 2021.

Good, S., Fiedler, E., Mao, C., Martin, M. J., Maycock, A., Reid, R., … Worsfold, M.: The current configuration of the OSTIA system for operational production of foundation sea surface temperature and ice concentration analyses, Remote Sensing,
1090   12(4), 1–20, https://doi.org/10.3390/rs12040720, 2020.

Graham, J. A., O'Dea, E., Holt, J., Polton, J., Hewitt, H. T., Furner, R., Guihou, K., Brereton, A., Arnold, A., Wakelin, S., Castillo Sanchez, J. M., and Mayorga Adame, C. G.: AMM15: a new high-resolution NEMO configuration for operational simulation of the European north-west shelf, Geosci. Model Dev., 11, 681–696, https://doi.org/10.5194/gmd-11-681-2018, 2018.

1095   Gurgel, K.-W., Schlick, T., Voulgaris, G., Seemann, J., and Ziemer, F.: HF radar observations in the German Bight: Measurements and quality control, IEEE/OES 10th Current, Waves and Turbulence Measurements (CWTM), 51–56. https://doi.org/10.1109/CWTM.2011.5759524, 2011.

Hasselmann, K., Barnett, T. P., Bouws, E., Carlson, H., Cartwright, D. E., Enke, K., Ewing, J. A., Gienapp, H., Hasselmann,

D. E., Kruseman, P., Meerburg, A., Muller, P., Olsbers, D. J., Richter, K., Sell, W., and Walden, H.: Measurements of wind-wave growth and swell decay during the joint North Sea wave project (JONSWAP), 1973. Retrieved from: https://repository.tudelft.nl/islandora/object/uuid:f204e188-13b9-49d8-a6dc-4fb7c20562fc?collection=research.

Hasselmann, S., Hasselmann, K., Allender, J. H., and Barnett, T. P.: Computations and Parameterizations of the Nonlinear Energy Transfer in a Gravity-Wave Specturm. Part II: Parameterizations of the Nonlinear Energy Transfer for Application in Wave Models, Journal of Physical Oceanography, 15(11), 1378–1391, https://doi.org/10.1175/1520-0485(1985)015<1378:CAPOTN>2.0.CO;2, 1985.

Hersbach, H., and Bidlot, J.-R.: The relevance of ocean surface current in the ECMWF analysis and forecast system, Workshop on Ocean-Atmosphere Interactions, Reading, United Kingdom, European Centre for Medium-Range Weather Forecasts, (November), 61–73, 2008.

Janssen, P. The Interaction of Ocean Waves and Wind. In The Interaction of Ocean Waves and Wind, https://doi.org/10.1017/cbo9780511525018, 2004.

King, R. R., While, J., Martin, M. J., Lea, D. J., Lemieux-Dudon, B., Waters, J., and O'Dea, E.: Improving the initialisation of the Met Office operational shelf-seas model. Ocean Modelling, 130(August), 1–14, https://doi.org/10.1016/j.ocemod.2018.07.004, 2018.

Lewis, H. W., Castillo Sanchez, J. M., Arnold, A., Fallmann, J., Saulter, A., Graham, J., Bush, M., Siddorn, J., Palmer, T., Lock, A., Edwards, J., Bricheno, L., Martínez-de la Torre, A., and Clark, J.: The UKC3 regional coupled environmental prediction system, Geosci. Model Dev., 12, 2357–2400, https://doi.org/10.5194/gmd-12-2357-2019, 2019.

Li, J.-G.: Hybrid multi-grid parallelisation of WAVEWATCH III model on spherical multiple-cell grids, Journal of Parallel and Distributed Computing, 167, 187–198, https://doi.org/10.1016/j.jpdc.2022.05.002, 2022.

Li, J. G.: Global transport on a spherical multiple-cell grid. Monthly Weather Review, 139(5), 1536–1555, https://doi.org/10.1175/2010MWR3196.1, 2011.

Li, J. G.: Propagation of ocean surface waves on a spherical multiple-cell grid, Journal of Computational Physics, 231(24), 8262–8277, https://doi.org/10.1016/j.jcp.2012.08.007, 2012.

Li, J. G., and Saulter, A.: Unified global and regional wave model on a multi-resolution grid, Ocean Dynamics, 64(11), 1657–1670, https://doi.org/10.1007/s10236-014-0774-x, 2014.

NOAA: WAVEWATCH III® Production Hindcast, Multigrid: Feb 2005 to May 2019, retrieved from https://polar.ncep.noaa.gov/waves/hindcasts/prod-multi_1.php, 2020.

Palmer, T., and Saulter, A.: Evaluating the effects of ocean current fields on a UK regional wave model, Met Office Research Technical Report No: 612, 2016. Retrieved from https://library.metoffice.gov.uk/Portal/Default/en-GB/DownloadImageFile.ashx?objectId=407&ownerType=0&ownerId=212801 (last access: 26/11/2022).

Piolle, J. F., Dodet, G., and Ash, E.: LOPS and CCI_Sea_state Team CCI+ Phase 1: Sea State cci Product User Guide, LOPS and Cci Sea State Team, 2020.

Saulter, A., Bunney, C., Li, J.-G., and Palmer, T.: Process and resolution impacts on UK coastal wave predictions from

operational global-regional wave models, 15th International Workshop on Wave Hindcasting and Forecasting and 6th Coastal Hazard Symposium, 2017. Retrieved from

http://www.waveworkshop.org/15thWaves/Papers/K1_WHF_SaulterEtAl_UKCoastalWave_20170913.pdf

Saulter, A. N., Bunney, C., King, R. R., and Waters, J.: An Application of NEMOVAR for Regional Wave Model Data Assimilation, Frontiers in Marine Science, 7(October), 1–19, https://doi.org/10.3389/fmars.2020.579834, 2020a.

Saulter, A.: North West European Shelf Production Centre - Quality Information Document, 1–60, 2020b. Retrieved from https://catalogue.marine.copernicus.eu/documents/QUID/CMEMS-NWS-QUID-004-014.pdf (last access: 26/11/2022).

Saulter, Andy, Bunney, C., and Li, J.: Application of a refined grid global model for operational wave forecasting, Forecasting Met Office Research Technical Report No: 614, 46, https://doi.org/10.13140/RG.2.2.22242.17600, 2016.

Siddorn, J. R., Good, S. A., Harris, C. M., Lewis, H. W., Maksymczuk, J., Martin, M. J., and Saulter, A.: Research priorities in support of ocean monitoring and forecasting at the Met Office, Ocean Science, 12(1), 217–231, https://doi.org/10.5194/os-12-217-2016, 2016.

Tolman, H. L.: User manual and system documentation of WAVEWATCH III® version 4.18, 2014. Retrieved from http://polar.ncep.noaa.gov/waves/wavewatch/manual.v4.18.pdf

Tonani, M, Pequignet, C., King, R., Sykes, P., Mcconnell, N., and Siddorn, J.: North West European Shelf Production Centre NORTHWESTSHELF_ANALYSIS_FORECAST_PHYS_004_013 Issue: 1.1. 1–46, 2021.

Tonani, M., Sykes, P., King, R. R., McConnell, N., Péquignet, A.-C., O'Dea, E., Graham, J. A., Polton, J., and Siddorn, J.: The impact of a new high-resolution ocean model on the Met Office North-West European Shelf forecasting system, Ocean Sci., 15, 1133–1158, https://doi.org/10.5194/os-15-1133-2019, 2019.

Valckle, S., Craig, T., and Coquart, L.: OASIS3-MCT User Guide, Cerfacs, Technical Report TR/CMGC/15/38, 2015.

Valiente, N. G., Saulter, A., Edwards, J. M., Lewis, H. W., Sanchez, J. M. C., Bruciaferri, D., Bunney, C., and Siddorn, J.: The impact of wave model source terms and coupling strategies to rapidly developing waves across the north-west european shelf during extreme events, Journal of Marine Science and Engineering, 9(4), https://doi.org/10.3390/jmse9040403, 2021a.

Valiente, N. G., Saulter, A., and Lewis, H. W.: The effect of different levels of coupling in surface wind waves along the NWS during extreme events, Met Office Forecasting Research Technical Report No:642, 2021b. Retrieved from https://digital.nmla.metoffice.gov.uk/IO_054d5518-86af-4a24-903d-fafa0d6a2695/ (last access: 26/11/2022).

Walters, D., Baran, A. J., Boutle, I., Brooks, M., Earnshaw, P., Edwards, J., Furtado, K., Hill, P., Lock, A., Manners, J., Morcrette, C., Mulcahy, J., Sanchez, C., Smith, C., Stratton, R., Tennant, W., Tomassini, L., Van Weverberg, K., Vosper, S., Willett, M., Browse, J., Bushell, A., Carslaw, K., Dalvi, M., Essery, R., Gedney, N., Hardiman, S., Johnson, B., Johnson, C., Jones, A., Jones, C., Mann, G., Milton, S., Rumbold, H., Sellar, A., Ujiie, M., Whitall, M., Williams, K., and Zerroukat, M.: The Met Office Unified Model Global Atmosphere 7.0/7.1 and JULES Global Land 7.0 configurations, Geosci. Model Dev., 12, 1909–1963, https://doi.org/10.5194/gmd-12-1909-2019, 2019.

Waters, J., Lea, D. J., Martin, M. J., Mirouze, I., Weaver, A., and While, J.: Implementing a variational data assimilation system in an operational 1/4degree global ocean model, Quarterly Journal of the Royal Meteorological Society, 141(687),

333–349. https://doi.org/10.1002/qj.2388, 2015.

Williams, K. D., Copsey, D., Blockley, E. W., Bodas-Salcedo, A., Calvert, D., Comer, R., Davis, P., Graham, T., Hewitt, H. T., Hill, R., Hyder, P., Ineson, S., Johns, T. C., Keen, A. B., Lee, R. W., Megann, A., Milton, S. F., Rae, J. G. L., Roberts, M.

1170   J., Scaife, A. A., Schiemann, R., Storkey, D., thorpe, L., Watterson, I. G., Walters, D. N., West, A., Wood, R. A., Woollings, T., and Xavier, P. K.: The Met Office Global Coupled Model 3.0 and 3.1 (GC3.0 and GC3.1) Configurations, Journal of Advances in Modeling Earth Systems, 10(2), 357–380, https://doi.org/10.1002/2017MS001115, 2018.

Young, I. R., and Verhagen, L. A.: The growth of fetch limited waves in water of finite depth. Part 1. Total energy and peak frequency, Coastal Engineering, 29, 47–78, 1996.

1175   WAVEWATCH III Development Group (WW3DG): User manual and system documentation of WAVEWATCH III® version 6.07. Tech. Note 333, NOAA/NWS/NCEP/MMAB, College Park, MD, USA, 465 pp. +Appendices, 2019.

Zieger, S.; Babanin, A.V.; Rogers, W.E.; and Young, I.R.: Observation-based source terms in the third-generation wave model WAVEWATCH, Ocean Model, 96, 2–25, doi:10.1016/j.ocemod.2015.07.014, 2015.